NVE

EKSTERN RAPPORT NR. 4 / 2025

Breaching of rockfill dams exposed to overtopping

Report R&D project 80418, part 2

SKREVET AV Théo Dezert og Fjóla G. Sigtryggsdóttir

NVE Ekstern rapport nr. 4/2025
Breaching of rockfill dams exposed to overtopping – Report R&D project 80418, part 2

Utgitt av:	Norges vassdrags- og energidirektorat
Redaktør:	Grethe Holm Midttømme (NVE)
Forfattere:	Théo Dezert og Fjóla G. Sigtryggsdóttir (NTNU)
Omslagsbilde:	Dambrudd ved Braskereidfoss kraftverk, 9.august 2023. Foto: Politiet/NVE

ISBN:	978-82-410-2458-0
ISSN:	2535-8235
Saksnummer:	202110167

Sammendrag: Rapporten gir en oppsummering av forskning på bruddforløp ved overtopping av fyllingsdammer. Hovedfokus er å teste empiriske formler for å estimere bruddparametere. Rapporten viser hvilke empiriske formler som gir best resultater, men også at formlene ikke er spesielt godt tilpasset typiske steinfyllingsdammer. De empiriske formlene tar ikke hensyn til erosjonssikring av stein på nedstrøms side, som er vanlig på norske steinfyllingsdammer. En forenklet erosjonsmodell er også testet, med gode resultater, men denne modellen krever mye inngangsdata (materialparametere mv) som ikke alltid er tilgjengelig.

Emneord: Fyllingsdam, damsikkerhet, bruddforløp, modellforsøk

Norges vassdrags- og energidirektorat
Middelthuns gate 29
Postboks 5091 Majorstuen
0301 Oslo

Telefon: 22 95 95 95
E-post: nve@nve.no
Internett: www.nve.no

Februar 2025

Forord

Siden 2013 har det vært utført omfattende forskning på fyllingsdammer ved NTNU, vassdragslaboratoriet i Trondheim. Det har resultert i flere doktoravhandlinger og Masteroppgaver, samt en rekke vitenskapelige artikler. Et hovedmål med FoU-prosjekt «Nedstrøms plastring, damtå og bruddforløp» har vært å få økt kunnskap om laster på nedstrøms plastring og damtå på steinfyllingsdammer, og om bruddforløp på steinfyllingsdammer med og uten plastring.

Arbeidene startet i 2022 som et post.doc-prosjekt utført av Théo Dezert. Prosjektleder har vært professor Fjóla Guðrún Sigtryggsdóttir. NVEs prosjektleder har vært Grethe Holm Midttømme.

I del 1 av prosjektet, som er presentert i NVE Ekstern rapport 12:2024, har det vært fokus på nedstrøms plastring og damtå. I del 2 av prosjektet, som er presentert i denne rapporten, har det vært fokus på bruddforløp for steinfyllingsdammer utsatt for overtopping. Rapporten bygger på laboratorieforsøk utført som del av doktorgradsprosjektet til Geir Helge Kiplesund ved NTNU (WP 1.2 HydroCen), samt tidligere storskala bruddforsøk utført som del av IMPACT-prosjektet (Korgenprosjektet) i 2002/2003 og studier av historiske dambrudd.

Resultatene fra prosjektet vil bidra til videreutvikling av veiledere og regelverk for fyllingsdammer, deriblant danne underlag for revisjon av damsikkerhetsforskriften.

Oslo, februar 2025

Andreu Regué Barrufet
seksjonssjef
Seksjon for damsikkerhet
Tilsyns- og beredskapsavdelingen

Dokumentet sendes uten underskrift. Det er godkjent i henhold til interne rutiner.

Sammendrag

Rapporten summerer opp og supplerer tidligere forskning på bruddforløp i fyllingsdammer med hovedfokus på empiriske formler for å estimere bruddparametere. Rapporten viser hvilke empiriske formler som gir best resultater, men også at formlene ikke er spesielt godt tilpasset typiske steinfyllingsdammer. De empiriske formlene tar ikke hensyn til erosjonssikring av stein på nedstrøms side, som er vanlig på norske steinfyllingsdammer.

Fyllingsdammer er sårbare for overtopping som kan føre til erosjon av fyllingsmassene. Det stilles flere krav til norske fyllingsdammer for å øke evnen til å motstå overtopping og redusere sannsynlighet for brudd, deriblant krav til erosjonssikring nedstrøms. Erosjonssikringen skal utføres som plastring som består av steiner plassert i forband, slik at steinene låses til hverandre. Selv om det stilles krav til sikring av fyllingsdammer for å unngå dambrudd, skal alle dammer klassifiseres med grunnlag i hvilke konsekvenser et eventuelt dambrudd kan få. Klassifiseringen avgjør hvilke krav som stilles til planlegging, bygging og drift av dammene. For dammene som havner i de høyeste konsekvensklassene er det også krav om å gjøre dambruddsbølgeberegninger som underlag for dameiernes beredskapsplaner og lokale myndigheters evakueringsplaner.

En vurdering av bruddkonsekvenser innebærer at det må gjøres estimater av teoretiske bruddvannføringer, som benyttes til å vurdere hvor stort område som kan bli oversvømt og hvilke områder som bør evakueres dersom dambrudd skjer. Gjeldende praksis er å bruke empiriske formler som bygger på data fra historiske dambrudd. Disse formlene tar ikke hensyn til damtype og - materialegenskaper, noe som fører til usikkerheter i resultatene. Denne rapporten fokuserer på å kvantifisere nøyaktigheten av bruddparametere (bruddbredde, bruddtid og bruddvannføring) fra ulike empiriske formler.

Resultater fra bruddforsøk på tre typer fyllingsdammer (homogen jordfyllingsdam, homogen steinfyllingsdam og soneinndelt steinfyllingsdam) testet under storskalaforsøkene i Korgen, Norge i 2002/2003 (IMPACT-prosjektet), samt informasjon fra fem historiske dambrudd, er benyttet for å evaluere de empiriske formlenes evne til å estimere bruddparameterne. I tillegg er fjorten laboratoriemodeller av steinfyllingsdammer (1:10 skala-modeller) fra doktorarbeidet til Geir Helge Kiplesund også benyttet. De fysiske laboratoriemodellene var utsatt for overtopping med økende vannføring til brudd.

Målte og estimerte bruddparametere er sammenlignet med mål om å identifisere hvilke av de empiriske formlene som passer best til forskjellige damtyper. Resultatene indikerer at de forskjellige empiriske formlenes egnethet til å estimere bruddparametere avhenger betydelig av egenskapene til dammen og tilhørende magasin.

For estimering av bruddbredde på dammer fra storskalaforsøk og historiske dambrudd, viser formlene foreslått av Xu & Zhang (2009) og Froehlich (2016a) de beste resultatene, mens formlene benyttet av U.S. Bureau of Reclamation (1988) ser ut til å være bedre for å beskrive bruddbredder fra laboratorietestene for modeller uten

erosjonssikring. Det presiseres at ingen av bruddformlene var egnet til å estimere bruddåpningen i de fysiske modellene som hadde erosjonssikring av stein (plastring eller rauset stein).

Froehlich (1995b) gir det beste estimatet av bruddtid for laboratoriemodeller med erosjonssikring av stein samt for storskala modellene og de historiske dambruddene. Xu & Zhang (2009) gir best estimat for laboratoriemodeller av steinfyllingsdammer uten erosjonssikring.

Froehlich (2016b) og Xu & Zhangs (2009) formler gir best estimat av bruddvannføringen for større magasiner samt for laboratoriemodeller uten erosjonssikring.

En forenklet fysisk basert bruddmodell (DLBreach) er også benyttet for å estimere bruddparametere for de tre storskala testdammene i Korgenprosjektet. En sammenligning med resultater fra de empiriske formlene er presentert. Resultatene fra DLBreach stemmer ganske bra overens med målinger, selv om bruddtiden ble overestimert for steinfyllingsdammene. En av ulempene med DLBreach er at den krever mer inngangsdata (materialparametere mv) enn de empiriske formlene.

Tilfredsstillende estimater av bruddparametere og forståelse av usikkerhetene i estimatene er viktig for damsikkerheten. Denne rapporten fremhever hvordan dam- og magasinegenskaper påvirker estimatene fra forskjellige bruddmodeller. Den viser også at det mangler gode bruddmodeller som er tilpasset fyllingsdammer med erosjonssikring.

Breaching of rockfill dams exposed to overtopping

NVE Project nr. 80418

Théo Dezert

Fjóla G. Sigtryggsdóttir

Department of Civil and Environmental Engineering

Norwegian University of Science and Technology

Trondheim,

2024

NTNU
Norwegian University of Science and Technology

NVE

Abstract

Embankment dams are hydraulic structures that can be exposed to extreme flood events, in turn leading to overtopping, which is the primary cause of embankment dam failure. These phenomena erode and affect structural and geotechnical integrity, which can induce dam breaching. Dam safety is a crucial consideration due to the potential for catastrophic consequences. Dam safety regulations and guidelines are increasingly demanding the enhancement of rockfill dams' resistance to overtopping and leakages. To protect against such erosion processes, ripraps are broadly used. Understanding their behavior during overtopping is one of the important issues to improve dam design and reinforcement techniques.

Assessing the breaching of embankments is also essential for conducting risk evaluations and hazard studies. Typically, this assessment is carried out using parametric breach models, which are statistically derived equations based on historical dam failure cases. However, these models often overlook important parameters like material properties, leading to uncertainties in the results. This research report focuses on quantifying the accuracy of breach parameters (breach width, failure time, peak outflow) predicted by various parametric breach models found in the literature.

Three prototype embankment dams (homogeneous earthfill dam, homogeneous rockfill dam, and zoned rockfill dam) from the IMPACT project, along with five historical failure cases, are considered to evaluate the predictive capability of the parametric breach models. Fourteen laboratory rockfill dam models (1:10 scale models), with or without riprap protection, are also considered and exposed to overtopping events with increasing discharge levels until complete failure. The experimental research in the laboratory was carried out as a part of Geir Helge Kiplesund‘s PhD work. This study compares the measured and estimated breaching parameter values, aiming to identify the most suitable parametric breach model based on the dam design.

The results indicate that the performance of the different models in estimating breach parameters significantly depends on the characteristics of the dam and reservoir. For breach width estimation at the prototype scale, the models proposed by Xu & Zhang (2009) and Froehlich (2016a) demonstrate the best accuracy while the U.S. Bureau of Investigation (1988) model appears to describe better the breach widths from laboratory tests on models without protection. Froehlich (1995b) provides the most reliable estimation for breach formation time for protected structures and dams at the prototype scale while Xu & Zhang (2009) provides the best estimation for unprotected rockfill dams carried out in the laboratory. Froehlich (2016b) finally offers the best estimation of peak outflow, particularly for larger reservoirs as well as for unprotected laboratory models along with Xu & Zhang's (2009) model. It is important to note that the quality of these estimations only stands for unprotected dams. Indeed, protected models (dumped or placed riprap) were poorly characterized. Additionally, a simplified physical model (DLBreach) is employed in this report to estimate breach parameters for the three prototype dams, and a comparison with results from parametric breach models is presented.

In conclusion, accurately predicting breach parameters is vital for improving dam safety as well as understanding the limitation of the prediction. This research report highlights the influence of dam and reservoir characteristics on the performance of different parametric breach models, and the inability of such models to describe breaching of dams with riprap erosion protection. By identifying the most suitable breach models for specific dam designs, this study contributes to the understanding and management of embankment dam failures.

Table of contents

Ph.D. thesis and work that are a part of the research projects at NTNU

Ph.D thesis

Priska H. Hiller (2017). Riprap design on the downstream slopes of rockfill dams. *Doctoral Thesis, Norwegian University of Science and Technology, Trondheim*.

Ganesh H.R. Ravindra (2020). Hydraulic and structural evaluation of rockfill dam behavior when exposed to throughflow and overtopping scenarios. *Doctoral Thesis, Norwegian University of Science and Technology, Trondheim*.

PhD work

The Ph.D. work by **Geir Helge Kiplesund** (2019 -) is a part of the research projects at NTNU and includes all the experimental work described in Chapter 4 of this report. The Chapter 4 is an adopted version of an article that will be a part of Geir Helge Kiplesund's PhD thesis.

MSc and Project thesis that are a part of the research projects at NTNU

A. 2017- 2022.

Guri Holte Veslegard (2017): *Plastring av fyllingsdammer - Modellforsøk, praktiske forhold og avvik fra regelverk,* (Master project).

Kofi Ntow Opare (2018) *Load measurements at riprap toe* (Master thesis).

Malin Fossum Asbølmo (2019) *Kartlegging av nedstrøms damtå på valgte fyllingsdammer/Field survey of downstream dam toes on selected rockfill dams* (Master project).

Malin Fossum Asbølmo (2019) *Utforming av damtå og betydning for plastring av fyllingsdammer - Kartlegging og modellforsøk/ Significance of toe support conditions on placed riprap stability- Field survey and model studies* (Master thesis).

Nils Solheim Smith (2020) *Physical and numerical modeling of extreme flow through rockfill dams* (Master thesis).

Styrmir Sigurjonsson (2020) *Breaching of rockfill dams* (Master thesis).

Ghaith Alkholossi (2021) *Rockfill dam breaching experiments with the application of photogrammetry techniques* (Master thesis)

Nisal Deelaka Halaba A. Senarathna (2021) *Effect of downstream erosion protection on the breaching of rockfill dams* (Master thesis).

Raj Kumar Kc (2022) *Experimental study into the overtopping and breaching of rockfill dams with erosion protection* (Master thesis).

Saroj Sapkota (2022) *Overtopping and breaching of rockfill dams with and without a central core* (Master thesis).

B. 2014-2016.

Ellen Bogfjellmo (2013): *Nedstrøms skråning av steinfyllingsdammer - Analyse av eksisterende plastringer. Development of a method to survey placed riprap on rockfill dams,* (Semester project).

Hans Edward Røer (2014): *Nedstrøms skråning av steinfyllingsdammer - Modellforsøk av plastring under ulike strømningsforhold. Scaled model tests of placed riprap exposed overtopping, through flow and a combination*, (Master thesis).

Ragnhild Sørlie Meaas (2014): *Plastring av elvebunn med sterk strøm. Scaled model tests of placed riprap exposed to supercritical flow,* (Master thesis).

Johannes Kobel (2014): *Smartstones. Testing out the Smartstone sensors and evaluating their application properties,* (Semester project).

Jens Jakobsen (2015): *Plastring av fyllingsdammer - Forskyving i plastring og anvendelse av Smartstone sensorer. Evaluating displacements in placed riprap and test the application of the Smartstone sensors,* (Master thesis).

Eirik Helgetun Pettersen (2015): *Plastring av fyllingsdammer - Effekt av forband på styrken av plastringen. The effect of interlocking placement on the stability of placed riprap,* (Master thesis).

Wiebke Marie Zander (2015): *Untersuchungen zur Genauigkeit von Smartstones - ein auf RFID-Technologie basierendes Tracersystem. Evaluating the accuracy of the Smartstone - a tracer system based on RFID technology,* (Bachelor thesis).

Fredrikke Kjosavik (2015): *Plastring av fyllingsdammer - Forskyvingar i damkrona. Analysis of displacements on the dam crest with large-scale field tests and scaled model tests,* (Master thesis).

Guri Holte Veslegard (2016): *Plastring av fyllingsdammer - Forskyving i plastring. Analysis of displacements within placed riprap,* (Semester project).

List of papers published as a part of the research projects at NTNU

A. 2018-2024

1. **Buckling analogy for 2D deformation of placed ripraps exposed to overtopping.** Ravindra, G.H.R., Sigtryggsdottir, F.G and Lia, L (2020). *Journal of Hydraulic Research,* DOI: https://doi.org/10.1080/00221686.2020.1744745.
2. **Toe support conditions for placed ripraps on rockfill dams- A field survey.** Ravindra, G.H.R., Sigtryggsdottir, F.G., Asbølmo, M.F and Lia, L (2019). *Vann* 2019 (3), pp. 185- 199. Retrieval link: https://vannforeningen.no/dokumentarkiv/toe-support-conditions-for-placed-ripraps-on-rockfill-dams-a-field-survey/
3. **Failure mechanism in placed riprap on steep slope with unsupported toe.** Ravindra, G.H.R., Gronz, O., Dost, B and Sigtryggsdottir, F.G. *Engineering Structures* 2020, Volume 221. DOI: https://doi.org/10.1016/j.engstruct.2020.111038
4. **Non-linear flow through rockfill embankments.** Ravindra, G.H.R., Sigtryggsdottir, F.G and Høydal, ØA (2019). *Journal of Applied Water Engineering and Research,* 7:4, 247-262. DOI: https://doi.org/10.1080/23249676.2019.1683085
5. **Effects of toe configurations on throughflow hydraulic properties of rockfill embankments.** Kiplesund, GH., Ravindra, G.H.R., Rokstad, M.M and Sigtryggsdottir, F.G (2021)**.** *Journal of Applied Water Engineering and Research*. DOI: https://doi.org/10.1080/23249676.2021.1884615
6. **Laboratory Investigations into Stability and Breaching of Rockfill Dams** Kiplesund, GH., Ravindra, Sigtryggsdottir, F.G (2021) *Publications of the Institute of Geophysics, Polish Academy of Sciences, C.*

7. **Numerical Modeling of the Effects of Toe Configuration on Throughflow in Rockfill Dams.**
Smith, N.S.; Ravindra, G.H.R.; Sigtryggsdottir, F.G.. (2021)
Water. vol. 13 (13). DOI: https://doi.org/10.3390/w13131726
8. **Placed Riprap Deformation Related to Axial Load at Toe Support: Physical Modelling.**
Dezert, T., Ravindra, G.H.R., Sigtryggsdóttir, F.G. (2022), In *Water*, *14*, 1581. *Water. 13(13), 1726.* DOI: https://doi.org/10.3390/w14101581
9. **Evaluation of design criteria for downstream riprap of rockfill dams.** Ravindra, G.H.R., Sigtryggsdottir, F.G., Lia, L (2018), Q. 101- R.71, pp. 1195- 1209, Twenty- sixth International Congress on Large Dams, 4th- 6th July, Vienna, Austria, Published by CRC Press, Taylor and Francis Group.
10. **Protection of embankment dam toe and abutments under overtopping conditions.**
Ravindra, G.H.R., Sigtryggsdottir, F.G., Lia, L (2018), 3rd International Conference on Protection against Overtopping, 6- 8 June, Grange over Sands, UK.
11. **Stability and failure mechanisms of riprap on steep slopes exposed to overtopping**.
Hiller, P.H., Ravindra, G.H.R (2020), In: Zhang JM., Zhang L., Wang R. (eds) Dam breach modeling and risk disposal. ICED 2020, Springer series in Geomechanics and Geoengineering. Springer, Cham.
12. **Riprap Protection Exposed to Overtopping Phenomena: A Review of Laboratory Experimental Models**
Dezert, T., Kiplesund, G. H., & Sigtryggsdóttir, F. G. (2022). Water, 14(17), 2722.
13. **Pertinence of parametric based breach models for rockfill dams.**
Sigurjónsson, S., Sigtryggsdóttir, F.G., Kiplesund, G. (2022), Proceedings of the 20th Int. Conf. On Soil Mechanics and Geotechnical Engineering, Sydney 2021.
14. **Riprap and rockfill dam experimental models exposed to overtopping events.**
Dezert, T., Ravindra, G.H.R., Sigtryggsdóttir, F.G. (2022), 27th ICOLD congress in Marseille, France, May 2022.
15. **Physical and numerical research on rockfill dams subjected to throughflow due to core overtopping.** Smith, N.S.; Kiplesund, G.H.; Ravindra, G.H.R.; Rokstad;

M.M., Sigtryggsdottir, F.G. (2022), 27th ICOLD congress in Marseille, France, May 2022.

16. **Load and deformation relations of placed riprap model with toe support.**
Dezert, T., Ravindra, G.H.R., Sigtryggsdóttir, F.G. (2022), 39th IAHR congress in Granada, Spain, June 2022.

17. **Laboratory investigations into stability and breaching of rockfill dams using dynamic Structure From Motion.**
Kiplesund, G.H., Sigtryggsdottir, F.G. (2022), 39th IAHR congress in Granada, Spain, June 2022.

18. **Riprap Protection Exposed to Overtopping Phenomena: A Review of Laboratory Experimental Models.**
Dezert, T., Kiplesund, G. H., & Sigtryggsdóttir, F. G. (2022), *Water*, *14*(17), 2722.

19. **Parametric breach models evaluation from laboratory rockfill dam overtopping.**
Dezert, T., Kiplesund, G. H., & Sigtryggsdóttir, F. G. (2023), 28th ICOLD congress in Goteborg, Sweden, June 2023.

20. **3D displacement and axial load of placed riprap supported at the toe: use of structure from motion.**
Dezert, T. & Sigtryggsdóttir, F. G. (2023), *Journal of Hydraulic Engineering, 150(1)*.

21. **Supported placed riprap exposed to overtopping: Structure from Motion Study.**
Dezert, T. & Sigtryggsdóttir, F. G. (2023), 40th IAHR congress in Vienna, Austria, August 2023.

22. **Evaluation of Parametric Breach Models from Prototype and Historical Embankment Dams under Overtopping Conditions.**
Dezert, T., & Sigtryggsdóttir, F. G. (2024), *Journal of Geotechnical and Geoenvironmental Engineering*, *150*(4).

23. **Parametric Breach Model Evaluation from Laboratory Rockfill Dam Models under Overtopping Conditions.**
Dezert, T., Kiplesund, G. H., & Sigtryggsdóttir, F. G. (2024). *Journal of Hydraulic Engineering, 150(6).*

B. 2014-2018

1. **Accumulating stone displacements as failure origin in placed riprap on steep slopes.**
   Priska H. Hiller, Jochen Aberle, *Journal of Hydraulic Research*, 2018, DOI: http://dx.doi.org/ 10.1080/ 00221686.2017.1323806
2. **Field and model tests of riprap on steep slopes exposed to overtopping.** Priska H. Hiller, Leif Lia, Jochen Aberle, *Journal of Applied Water Engineering and Research, 2018*. DOI: https://doi.org/10.1080/23249676.2018.1449675
3. **Smartstones: A small 9-axis sensor implanted in stones to track their movements.**
   Oliver Gronz, Priska H. Hiller, Stefan Wirtz, Kerstin Becker, Thomas Iserloh, Manuel Seeger, Christine Brings, Jochen Aberle, Markus C. Casper, Johannes B. Ries (2016) *CATENA*: 142, 245-251, Doi: http:// dx.doi.org/ 10.1016/ j.catena.2016.03. 030.
4. **Placed riprap as erosion protection on the downstream slope of rockfill dams exposed to overtopping.**
   Priska H. Hiller, Leif Lia, *25th Congress on Large Dams Stavanger*, Norway, 2015.
5. **Dam Svartevatn - An example of challenging upgrading of a large rockfill dam.**
   Priska H. Hiller, Leif Lia, Per Magnus Johansen, Rolv Guddal*, ICOLD Annual Meeting and Symposium* Bali, Indonesia, 2014.
6. **Riprap design on the downstream slope of rockfill dams.**
   Priska H. Hiller, Leif Lia, Jochen Aberle, Stefan Wirtz, Markus C. Casper Mitteilungen - Leichtweiss-Institut für Wasserbau der Technischen Universität Braunschweig Vol. 161, 39-44, 2014.
7. **Large-scale overtopping tests - Practical challenges and experience**.
   Priska H. Hiller, Leif Lia, *1st International Seminar on Dam Protections against Overtopping and Accidental Leakage,* Madrid, Spain, 2014.
8. **Practical challenges and experience from large-scale overtopping tests with placed riprap.**
   Priska H. Hiller, Leif Lia (2015), In M. Á. Toledo, R. Morán, E. Oñate (Eds*.), Dam Protections against Overtopping and Accidental Leakage*, 151-157. London: CRC Press/ Balkema.

9. **Field tests of placed riprap as erosion protection against overtopping and leakage**.

   Priska H. Hiller, Fredrikke Kjosavik, Leif Lia, Jochen Aberle, *United States Society on Dams - Annual Meeting and Conference Denver* CO, USA, 2016.

10. **Kartlegging av plastring på nedstrøms skråning av fyllingsdammer**. Survey of placed riprap on the downstream slopes of rockfill dams, Priska H. Hiller NTNU Report B1-2016-1, ISBN-10: 978-827598-095-1 Trondheim, Norway, 2016.

List of Figures

List of Tables

1 Introduction

Embankment dams encompass both earthfill and rockfill dams and stand for 78% of all dams in the world (ICOLD 1995). The difference between what is defined as a rockfill dam and an earthfill dam lies in the content of fine and coarse-grained material in the structure. In Norway, especially, rockfill dams are very commonly used and represent more than half of the 360 large dams (over 15 m high) present in the country. As stated by the International Commission on Large Dams (ICOLD), the primary cause of embankment dam failure is the overtopping mechanism. Overtopping accounts for approximately 40% of all cases where embankment dams have failed (ICOLD 2021). Given the catastrophic consequences associated with the breaching of a large dam, ensuring dam safety is of utmost importance.

During the process of overtopping, the downstream slope of a dam experiences highly destabilizing dynamic forces. These forces are generated by two mechanisms: turbulent overflow, which occurs when the crest is overtopped, and excessive throughflow, which happens when the core of the dam is overtopped. In the case of throughflow, the high-velocity turbulent flow within the dam may trigger internal erosion processes and also destabilizes the downstream embankment due to an increase in pore pressure. If the crest is overtopped, the downstream slope becomes submerged under turbulent surface flow, resulting in external erosion processes that can ultimately lead to a dam breach.

Hence, equipping dams with defense mechanisms to safeguard the structure against unanticipated overtopping or leakage events is important from a dam safety perspective. Ripraps are one of the most widely used erosion protection measures for various in-stream hydraulic structures such as embankment dams, spillways, streambeds, river banks, bridge piers, and abutments (e.g. Hiller et al., 2019; Thornton et al., 2014; Abt et al., 2013; Khan & Ahmad, 2011; Siebel, 2007). Ripraps are also used in coastal protection structures such as dikes, embankments, and jetties against wave action (Kobayashi & Jacobs, 1985). As applied to rockfill dam engineering, ripraps are constructed on the upstream embankment to protect against erosion resulting because of wave impacts and ice-induced forces. Further,

ripraps are constructed on the downstream slope to protect against erosion due to accidental leakage or overtopping events.

In the field, two main types of riprap structures can be encountered on rockfill dams: dumped riprap and placed riprap. The difference between these two structures lies in the construction technique. While dumped riprap are composed of stones placed randomly on the dam shoulder, placed riprap correspond to an arrangement of stones that follow an interlocking pattern. Owing to this specific arrangement, placed riprap is more resistant to overtopping events (Hiller et al., 2018; Ravindra et al., 2020) even though setting up such structures remains more expensive than dumped riprap from an economic standpoint.

Abt and Thornton (2014) detailed the advances in research on riprap design for overtopping, mentioning important authors and works such as Siebel (2007), Olivier (1967), Stephenson (1979), Abt and Johnson (1991) and Khan and Ahmad (2011). Moreover, Najafzadeh and Oliveto (2020) used experimental datasets from many authors to assess the performance of artificial intelligence techniques to predict critical overtopping discharge values for riprap failure. Their results demonstrate that the stone-related Froude number is mainly controlled by the dam slope. However, most of these works only display research on dumped riprap on moderate slopes ($S < 0.5$). As detailed in Ravindra (2020), failure mechanisms differ a lot from dumped to placed riprap exposed to overtopping.

For embankment dams exposed to overtopping, many dam failures have been analyzed in the literature to propose parametric breaching equations from regression analysis to estimate breaching parameters such as (i) breach width, (ii) breach formation time, and (iii) peak outflow. The average breach width is defined as one-half of the sum of the trapezoid top width and bottom width of the breach (U.S. Bureau of Reclamation 1988; Froehlich 1995a; Froehlich 2008; Xu & Zhang 2009; Froehlich 2016a). The breach formation time is the time needed for the complete development of the breach following the initiation phase (MacDonald & Langridge-Monopolis 1984; U.S. Bureau of Reclamation 1988; Froehlich 1995b; Froehlich 2008; Xu & Zhang 2009; Froehlich 2016a) while the peak outflow corresponds to the maximum flow rate during the breaching phenomenon (Soil Conservation Service 1981; Singh and Snorrason 1982 and 1984; U.S. Bureau of Reclamation 1982; Costa 1985; Evans 1986; Froehlich 1995b; Walder & O'Connor 1997; Pierce 2008; Xu & Zhang 2009; Froehlich 2016b). All these parametric breach models are derived from multiple historical failure cases associated with many different dam types, designs, and dimensions.

Thus, the uncertainties associated with the estimations they provide can be quite important and there is no agreement on which equation should be used preferably. This research report focuses on introducing the parametric breach models and on comparing their ability to estimate the breaching parameters from multiple real cases (three prototype dams that are part of the European IMPACT project: Investigation of Extreme Flood Processes and Uncertainty and five historical dams). However, as there are very few breaches of rockfill dams that have been recorded, there is very limited data available to verify the validity of empirical breach equations for these dams. Thus, the research described here is also an attempt to use fourteen laboratory breach tests of rockfill dam models with steep slopes, with and without riprap protection, to validate existing parametric breach models and provide some guidance on which models perform better for these types of dams.

1.1 Research at NTNU

Experimental and analytical studies on rockfill dams subjected to throughflow and overtopping have been conducted at the Department of Civil and Environmental Engineering at NTNU, Trondheim, for over a decade. The work has been carried out in three main research projects, starting with PlaF in 2013 (Development of a tool for optimal riprap protection of rockfill dams), continuing in 2017 in the research center HydroCen within project WP1.2 Dams and dam safety and finally in 2021 within a postdoctoral project associated with WP1.2 of HydroCen. Professor Leif Lia was the project manager for PlaF. Professor Fjóla G. Sigtryggsdóttir is the project manager for project WP1.2 Hydrocen and the postdoctoral project.

This report is written as a part of the postdoctoral project that is funded by NVE (50%) and the hydropower industry (50%) through the contribution of Hafslund E-CO Vannkraft, Hydro Energi, NEAS, SFE Produksjon, Sira-Kvina, Skagerak Kraft AS, Statkraft, Tafjord Kraftproduksjon, and Trønder Energi. NVE Ekstern rapport nr. 17/2021 (Ravindra and Sigtryggsdóttir, 2021) summarizes the main findings from the first two research projects with work conducted from 2014 to 2020, while NVE Ekstern rapport nr. 12/2024 (Dezert and Sigtryggsdóttir, 2024b) presents further results from these research projects as well as new experimental work carried out in 2022. The present technical report presents work relating to breaching rockfill dam carried out within WP1.2 HydroCen through the PhD work

of Geir Helge Kiplesund, as well as within the postdoctoral project. A summary of scaled critical discharge values, from all experimental rockfill dam models under overtopping conditions carried out at NTNU, is also displayed in Appendix A.

The master theses and finalized PhD theses associated with the above-mentioned research projects are listed on pages 6 to 12, along with journal publications and conference articles. The Ph.D. thesis within these research projects are those of Priska H. Hiller in PlaF and Ganesh H.R. Ravindra in WP1.2 HydroCen (A1.2.1). Additionally, publications that are a part of the ongoing Ph.D. work of Geir Helge Kiplesund in WP1.2 HydroCen (A.1.2.2) are listed, as well as publications relating to the ongoing postdoctoral project in WP1.2 HydroCen of the first author of this report, Théo Dezert.

1.2 Scope and objectives of this present report

Many experimental and analytical studies conducted at the Department of Civil and Environmental Engineering at NTNU (Trondheim) have been directed towards investigating failure mechanisms in rockfill dam models subjected to throughflow and/or overtopping conditions. This present report aims at achieving a better understanding of breach development of embankment dams exposed to overtopping from laboratory experiments as well as prototype dams and historical failure cases.

First, the parametric breach models available in the literature are introduced in **Chapter 2** of this technical report, along with the description of the breach parameters required to use them. The breaching parametric equations are detailed for the three following breaching parameters: breach width, breach formation time, and peak outflow.

Then, in **Chapter 3**, the three prototype dams (from the IMPACT project) with their material properties as well as the five historical failure cases (Banqiao, Shimantan, Butler Valley, Oros, and Cougar Creek) are introduced. The data acquisition protocol is described for the IMPACT prototype dams and the input parameter values are displayed for all dam cases. The measured and estimated breaching parameters are presented and discussed according to the input parameters and the dam design. Particularly, the important limitations of this study and parametric models are highlighted. The simplified physical model DLBreach is also

briefly introduced to display and compare the results obtained on the prototype dams. The Chapter 3 bases on the work presented by Dezert and Sigtryggsdóttir (2024a).

Chapter 4 is focused on laboratory rockfill dam models. It is structured in the same manner as the previous chapter. The fourteen experimental models (unprotected, with placed, or with dumped riprap) are introduced as well as the data acquisition protocol. The breaching parameters measured and estimated are displayed and the suitability of the parametric breach models is discussed according to the type of setup. Chapter 4 bases on the work presented by Dezert et al. (2024), embracing experimental work carried out as a part of the PhD work of Geir Helge Kiplesund in WP1.2 HydroCen.

Finally, a concluding summary is provided in **Chapter 5**, putting into perspective the obtained results from these two new comparative studies.

The present report is prepared in compliance with a contract between NVE and NTNU on project nr. 80418 in NVE registry, with the Norwegian title “Plastring, damtå og bruddforløp for fyllingsdammer” or “Riprap, dam toe, and breaching of embankment dams”. This report is part of a research project at NTNU conducted within WP1.2 HydroCen.

2 Breaching of embankment

2.1 Breaching parameters

According to Morris et al. (2009), the breach of a dam is mainly influenced by two parameters: the dam's structure, including design, geometry, material properties, and the hydraulic load. Additionally, the conditions present in the reservoir play a central role in determining the size and growth of the breach. Many parametric equations have been developed to describe the geometric and hydrographic parameters involved in breach development, including average breach width (B_{avg}), breach formation time (t_f), and peak outflow (Q_p). These equations are statistically derived from regression equations based on historical dam failures. Some authors consider failure cases from all types of dams, while others focus on specific designs or use unique geometrical parameters. The input parameters for such equations are mainly geometric (Figure 1), including h_d, the dam height; h_b, the final breach depth; h_w, the height of water above the breach bottom when the failure starts; and W_{avg}, the average width of the embankment above breach bottom. However, hydraulic parameters such as V_w, the volume of water when the failure starts, and S, the reservoir's capacity, are also considered in some equations.

2.2 Breaching parametric equations

In this research work, we consider 31 equations (Eqs. 1-31) to estimate geometric and hydrographic B_{avg}, t_f, and Q_p. An overview of these equations is displayed in Tables 1-3. Several publications have proposed equations for estimating breach parameters based on data collected from dam failures. If we look at them chronologically, the Soil Conservation Service (1981) proposed a relationship between h_w and Q_p (Eq. 14) based on 13 embankment dam failures. Singh and Snorrason (1982) and (1984) analyzed eight earthfill dam failures caused by overtopping and proposed equations (Eqs. 15 and 16) for estimating Q_p based on H_d and S values. MacDonald & Langridge-Monopolis (1984) used data from 42 embankment dam failures to develop parametric equations for estimating t_f (Eqs. 7 and 8) and Q_p (Eq. 17) for both earthfill dams and non-earthfill dams (rockfill embankments, embankments with protective concrete surface layers, and embankments with core walls)

using h_w and V_w values. Costa (1985) gathered data from 31 cases of failure from all types of dams (rockfill, earthfill, and concrete dams) and provided best-fit equations for the estimation of Q_p (Eqs. 19 and 20) from V_w and h_d values. Evans (1986) used data from 11 embankment dam failures taken from MacDonald & Langridge-Monopolis (1984) study to introduce a best-fit empirical logarithmic relationship between Q_p and V_w (Eq. 21). The U.S. Bureau of Reclamation (1988) proposed parametric equations for identifying downstream hazards and assigning a dam hazard classification. The equations were defined for both earthfill and rockfill dams, relying on the use of h_w values (Eqs. 1 and 2).

Froehlich (1995a) then analyzed data from 63 embankment dam failures caused by overtopping or piping and proposed empirical models of breach formation. Based on these models, Froehlich (1995a) developed equations for estimating B_{avg} (Eq. 3) and t_f (Eq. 10) using V_w and h_b values. Froehlich (1995b) also estimated Q_p (Eq. 22) from V_w and h_w values. Froehlich (2008) and Froehlich (2016a) updated these formulas with data from 74 (Eqs. 4 and 11) and 111 (Eqs. 6, 13, and 31) embankment dams, respectively, mainly earthfill dams. Walder & O'Connor (1997) displayed three equations (Eqs. 23, 24, and 25) obtained from regression relations to estimate Q_p for constructed dams (rockfill, earthfill, and concrete dams) from h_w and V_w values. Pierce (2008) gathered data from 87 cases of embankment dam failures and developed multiple regression equations (Eqs. 26, 27, 28, and 29) to predict Q_p based on h_w and V_w values. Finally, Xu and Zhang (2009) proposed empirical equations that consider physical factors such as dam design, failure mode, and material erodibility to predict embankment dam breach parameters for different types of dams. They collected data from 182 failure cases across eight countries, mainly China and the United States. The parametric equations (Eqs 5, 12, and 30) use three parameters: B3, B4, and B5, which are determined by adding three values for each dam type, failure mode, and material erodibility. $B_3 = b_3 + b_4 + b_5$ where b_3 is -0.041, 0.026, or -0.226 for dams with corewalls, concrete-faced dams, or homogeneous/zoned dams; $b_4 = 0.149$ for overtopping and -0.389 for piping failure mode; b_5 = 0.291, -0.140 or -0.391 for high, medium or low erodibility materials. $B_4 = b_3 + b_4 + b_5$ where b_3 is -0.503, -0.591, or -0.649 for dams with corewalls, concrete-faced dams, or homogeneous/zoned dams; $b_4 = -0.705$ for overtopping and -1.039 for piping failure mode; $b_5 = -0.007$, -0.375 or -1.362 for high, medium or low erodibility materials. $B_5 = b_3 + b_4 + b_5$ where b_3 is -0.327, -0.674, or -0.189 for dams with corewalls, concrete-

faced dams, or homogeneous/zoned dams; b_4 = -0.579 for overtopping and -0.611 for piping failure mode; b_5 = -1.205, -0.564 or 0.579 for high, medium or low erodibility materials.

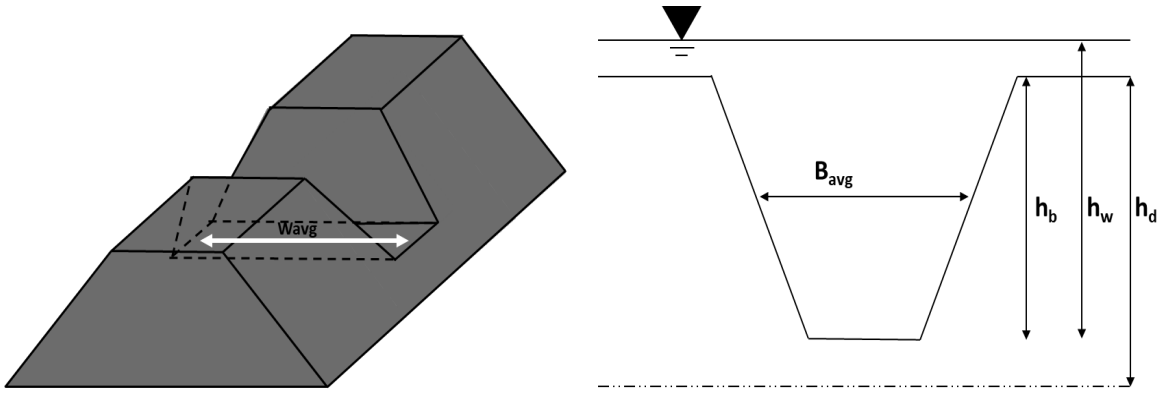

Figure 1. Left figure: representation of W_{avg} (Dezert and Sigtryggsdóttir, 2024a). Right figure: dimension of a final trapezoidal dam breach, modified from Froehlich (1995a).

Table 1. Breach width equations, B_{avg} (m), for overtopping homogenous/zoned dams and medium erodibility material. $\boldsymbol{V_w}$ is expressed in m^3 while $\boldsymbol{h_w}$, $\boldsymbol{h_b}$, $\boldsymbol{h_d}$ are expressed in m.

Reference	Type of dams	Equation	Equation number
U.S. Bureau of Reclamation (1988)	Earthfill	$3\ h_w$	(1)
U.S. Bureau of Reclamation (1988)	Rockfill	$2.5\ h_w$	(2)
Froehlich (1995a)	Embankment	$21\ (V_w 10^{-6})^{0.32} h_b^{\ 0.19}$	(3)
Froehlich (2008)	Embankment	$0.351\ V_w^{\ 0.32} h_b^{\ 0.04}$	(4)
Xu & Zhang (2009)	Embankment	$0.787\ h_b \left(\frac{h_d}{15}\right)^{0.133} \left(\frac{V_w^{\ 1/3}}{h_w}\right)^{0.652} e^{B_3}$	(5)
Froehlich (2016a)	Embankment	$0.345\ V_w^{\ 1/3}$	(6)

Table 2. Breach formation time equations, t_f (hrs), for overtopping homogenous/zoned dams and medium erodibility material. $\boldsymbol{V_w}$ is expressed in m^3 while $\boldsymbol{h_w}$, $\boldsymbol{h_b}$, $\boldsymbol{h_d}$, $\boldsymbol{B_{avg}}$ are expressed in m.

Reference	Type of dams	Equation	Equation number
MacDonald & Langridge-Monopolis (1984)	Earthfill	$0.00475(V_w H_w)^{0.31}$	(7)
MacDonald & Langridge-Monopolis (1984)	Non-earthfill	$0.00228(V_w H_w)^{0.28}$	(8)
U.S. Bureau of Reclamation (1988)	Earthfill and rockfill	$0.00684\ B_{avg}$	(9)
Froehlich (1995a)	Embankment	$3.84\ (V_w 10^{-6})^{0.53}\ h_b{}^{-0.9}$	(10)
Froehlich (2008)	Embankment	$0.01756\sqrt{\frac{V_w}{g h_b^2}}$	(11)
Xu & Zhang (2009)	Embankment	$0.304\left(\frac{h_d}{15}\right)^{0.707}\left(\frac{V_w{}^{1/3}}{h_w}\right)e^{B_5}$	(12)
Froehlich (2016a)	Embankment	$0.017\sqrt{\frac{V_w}{g h_b^2}}$	(13)

Table 3. Peak outflow equations, Q_p (m^3/s), for overtopping homogenous/zoned dams and medium erodibility material. S and $\boldsymbol{V_w}$ are expressed in m^3 while $\boldsymbol{h_w}$, $\boldsymbol{h_b}$, $\boldsymbol{h_d}$, $\boldsymbol{W_{avg}}$ are expressed in m.

Reference	Type of dams	Equation	Equation number
Soil Conservation Service (1981)	Embankment	$16.6\ h_w^{1.85}$	(14)
Singh and Snorrason (1982)	Earthfill	$13.4\ h_d^{1.89}$	(15)
Singh and Snorrason (1984)	Earthfill	$1.776\ S^{0.47}$	(16)
MacDonald & Langridge-Monopolis (1984)	Earthfill	$1.154\ (V_w H_w)^{0.412}$	(17)
U.S. Bureau of Reclamation (1982)	All types	$19.1\ h_w^{1.85}$	(18)
Costa (1985)	All types	$1.122\ (V_w)^{0.57}$	(19)
Costa (1985)	All types	$0.981\ (V_w h_d)^{0.42}$	(20)
Evans (1986)	Embankment	$0.72\ {V_w}^{0.53}$	(21)
Froehlich (1995b)	Embankment	$0.607\ V_w^{0.295} h_w^{1.24}$	(22)
Walder & O'Connor (1997)	Constructed	$1.16\ (h_w)^{0.46}$	(23)
Walder & O'Connor (1997)	Constructed	$2.5\ (h_w)^{2.34}$	(24)
Walder & O'Connor (1997)	Constructed	$0.61\ (h_w V_w)^{0.43}$	(25)
Pierce (2008)	Embankment	$0.0176\ (V_w h_w)^{0.606}$	(26)
Pierce (2008)	Embankment	$0.038 (V_w)^{0.475} (h_w)^{1.09}$	(27)
Pierce (2008)	Embankment	$0.784\ (h_w)^{2.668}$	(28)
Pierce (2008)	Embankment	$0.00919\ (V_w)^{0.745}$	(29)
Xu & Zhang (2009)	Embankment	$0.175 \sqrt{g V_w^{5/3}} \left(\frac{h_d}{15}\right)^{0.199} \left(\frac{{V_w}^{1/3}}{h_w}\right)^{-1.274} e^{B_4}$	(30)
Froehlich (2016b)	Embankment	$0.0324 \sqrt{\frac{g V_w h_w h_b^2}{W_{avg}}}$	(31)

3 IMPACT Project

This chapter is an adapted version of Dezert and Sigtryggsdóttir (2024a).

3.1 Dam descriptions

The experimentation considered in this chapter is part of the European IMPACT project: Investigation of Extreme Flood Processes and Uncertainty and complementary information can be found in the two dedicated reports (EBL Kompetanse 2006 and Morris 2009). The experimental site is located in the middle of Norway, close to Mo i Rana municipality (see map Figure 2). It is located about 600 m downstream of Røssvassdammen dam (Figure 2). The inflow to the reservoir upstream of the experimental dam could be regulated using the spillway gates from Røssvassdammen dam, with a maximum capacity of around 450 m^3/s when the dam is at the full supply level. The inflow was different for all prototype dams and was adapted to keep the water level in the reservoir during the overtopping stage. Three prototype dams are considered in this research and detailed in the following sections (Tests 1-2002, 2-2002, and 1-2003). A shallow pilot channel was present in the center of the three test dam crests to ensure that the overtopping failure started in the middle of the dam and not towards the abutments. Two water level gauges, VM1 and VM2, were positioned upstream of the prototype dams to monitor the water level in the reservoir, while two other gauges, VM3 and VM5, were installed downstream of the test embankment to measure the discharge from the test site. The locations of these gauges are displayed in Figure 2. The discharge was measured at VM5, located 230 meters downstream of the prototype dam site. The description of the failure process for all three cases is proposed hereafter and was mainly inspired by the descriptions detailed in EBL Kompetanse (2006).

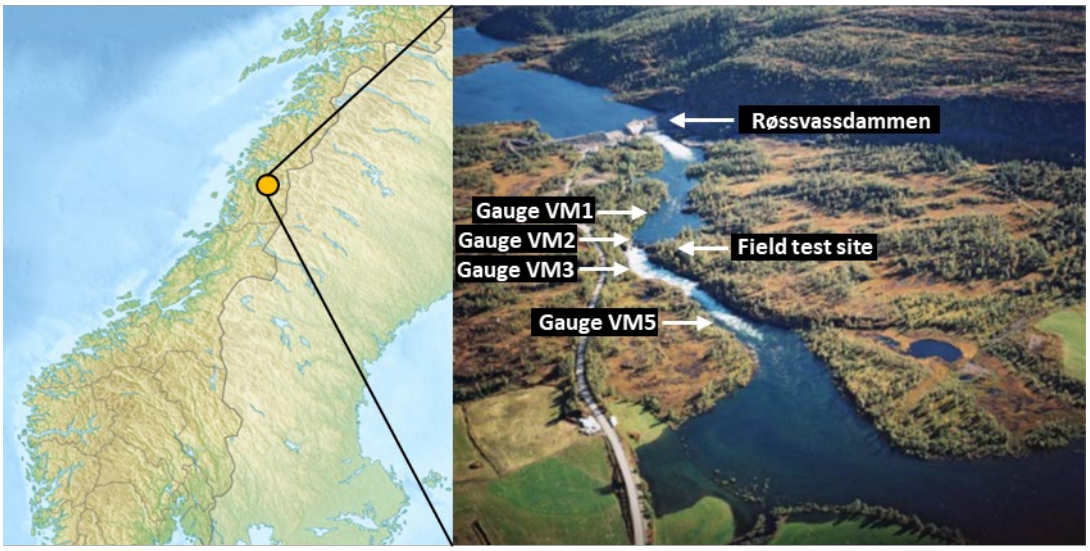

Figure 2. Field test site location, adapted from Vaskinn et al. (2004).

3.1.1 Field Test T1-2002

The first experimental test (T1-2002) is a homogeneous cohesive clay dam, exposed to overtopping on the 12th of September 2002. A pilot channel (6.66 × 0.45 m) is present in the center of the crest and a cross-section of the dam is displayed in Figure 3 to highlight the design and dimensions of the prototype dam. The material properties are displayed in Table 4. During the construction, dozer compaction of clay in 0.15 m layers was carried out. However, high water content and rainy weather made dam construction difficult. The compaction layer thickness was increased to 0.4 m and compaction pressure was reduced to improve construction speed. This resulted in two layers of clay with different erodibility. During testing, the upstream water level control was difficult, causing periodic overflow across the left side of the embankment crest and seepage developed along the left abutment. Breach initiation occurred in the central part of the embankment, within the pilot channel. The erosion concentrated in surface irregularities and loose lumps of clay were picked up, resulting in irregular erosion at the dam toe. The flow developed a horizontal crack along the lower right part of the overtopped dam face, forcing about half of the discharge mainly to the right. The erosion at the crack continued to expand and deepen, forcing more flow to the right, and developed into one single head cut progressing upstream. The erosion process in the breach opening was sporadic, with the sides undercutting, the clay cracking and slumping into the flow, and the process repeating itself.

Table 4. Material properties of prototype dam T1-2002 (Morris, 2009).

Moisture content	30
D50 (mm)	0.007
Porosity	0.46
Friction angle	22.9
Grain density ($g.cm^{-3}$)	2.8
Cohesion ($kN.m^{-2}$)	4.9
Dry density ($kN.m^{-3}$)	14.8

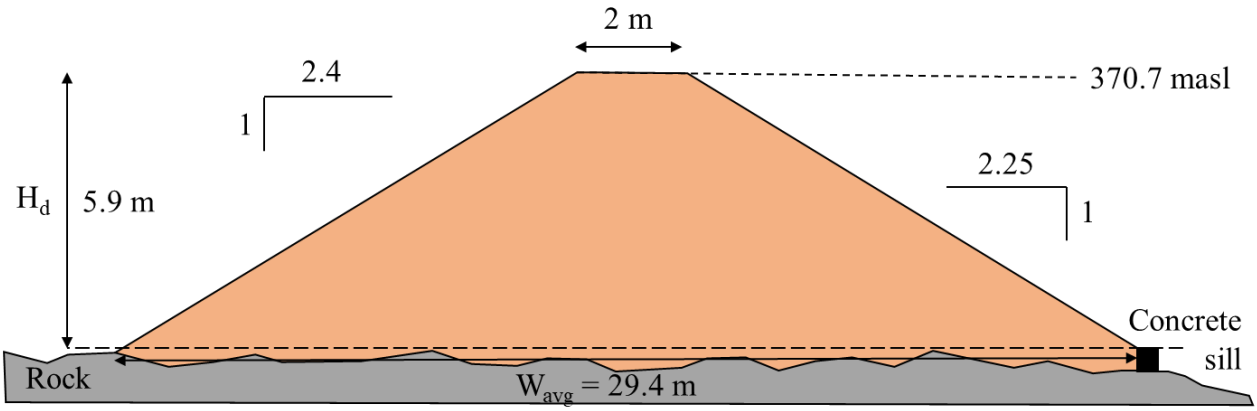

Figure 3. Test 1-2002, homogeneous cohesive clay dam.

3.1.2 Field Test T2-2002

The second experimental test (T2-2002) is a homogeneous gravel dam exposed to overtopping on the 16th of October 2002. A pilot channel (2 × 0.12 m) is present in the center of the crest and a cross-section of the dam is displayed in Figure 4 to highlight the design and dimensions of the prototype dam. The material properties are displayed in Table 5. The gravel embankment was created by compacting 0.5 m layers with a vibratory roller. On the 15th of October, the reservoir was filled to saturate the dam body until the breach test began the following day. Unfortunately, for that specific test, there was frost overnight, resulting in a frozen layer a few centimeters thick on the crest of the dam. The frozen layer was thinner on the downstream face and decreased towards the toe where water seeped out. To defrost the surface layer of the pilot channel, sandbags, and a plank were used to block the downstream edge of the channel and allow the upstream water level to rise and flood the crest area of the dam. Initially, during overtopping, surface erosion occurred downstream of

the crest, but it soon developed into head cuts at the toe, creating waterfalls while working itself upstream towards the reservoir. The erosion on the downstream side had a head-cut characteristic, similar to the one experienced in Test 1-2002. A few minutes before the breach formation, the erosion started cutting into the crest. The breach formation phase was not affected by the frozen dam crest as erosion took place in the upstream face and the dam body. The reservoir level fell rapidly, and the erosion process was much more continuous than for the clay dam. The slumping of material from the almost vertical sides of the breach opening was frequent and of small volumes.

Table 5. Material properties of prototype dam T2-2002 (Morris, 2009).

Moisture content	7
D50 (mm)	4.75
Porosity	0.22
Friction angle	42
Grain density (g.cm^{-3})	2.77
Cohesion (kN.m^{-2})	0.9
Dry density (kN.m^{-3})	21.2

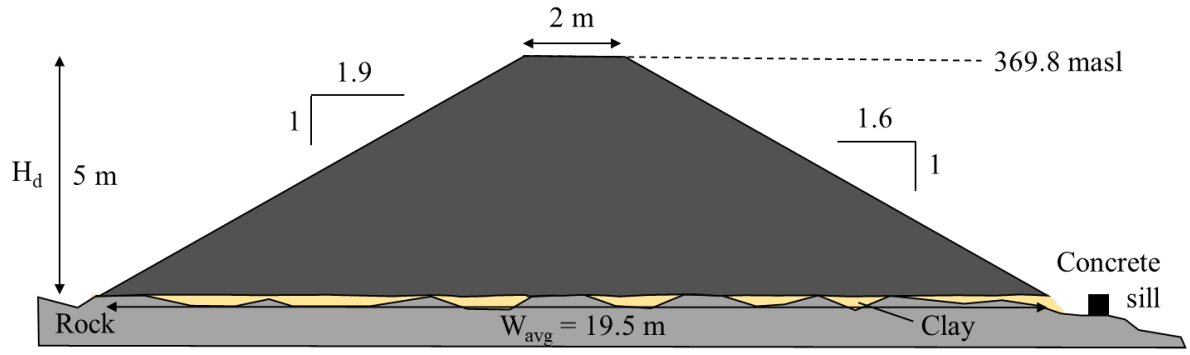

Figure 4. Test 2-2002, homogeneous gravel (0 – 60 mm) dam.

3.1.3 Field Test T1-2003

The third experimental test from the IMPACT project (T1-2003) is a zoned rockfill moraine core dam. This prototype dam was exposed to overtopping on the 21st of August 2003. A pilot channel (6.5 × 0.24 m) was present in the center of the crest and a cross-section of the dam is displayed in Figure 5 to highlight the design and dimensions of the prototype dam. The moraine core and rockfill properties are displayed in Table 6. The moraine core was

compacted with a vibratory roller in 0.5 m layers. The rock fill used was well-graded and came from tunnel spoil ranging from 0 – 500 mm and was compacted in 1 m layer thicknesses. In addition, uniform rock fill of 300 – 400 mm was also used and compacted in 1 m layer thicknesses (Figure 5). The reservoir was filled to saturate the dam body from the 19th of August. During the overtopping test, the seepage first emerged mostly at the dam toe, but some seepage was then seen in the dam. The seepages flushed away some fines and then the erosion stopped. During the overtopping, the water level was raised six times, resulting in three levels within the pilot channel and three levels overtopping the dam crest. As water flowed out of the pilot channel, it formed minor gullies that transported material to the end of the gully where most of it was deposited. This process resulted in small cascades dissipating energy along the dam face. As the discharge increased, the upper gullies moved further downstream, increasing the gradient and erosion of the upper gullies while protecting the lower gullies or dam toe. With a further increase in discharge, the upper gullies developed into one single waterfall, eroding into the dam body and moving the material further down the dam toe. Besides erosion in the gullies, the water started eroding on the dam crest at the bottom of the pilot channel. The cohesion in the moraine core caused the fill to slump more frequently than the core, resulting in larger slumps and a more irregular erosion process. When part of the core got exposed and collapsed, it rapidly increased the breach discharge. The maximum reservoir elevation was reached at the same time. Then, the reservoir level fell rapidly. The breach that formed was almost as wide as the pilot channel.

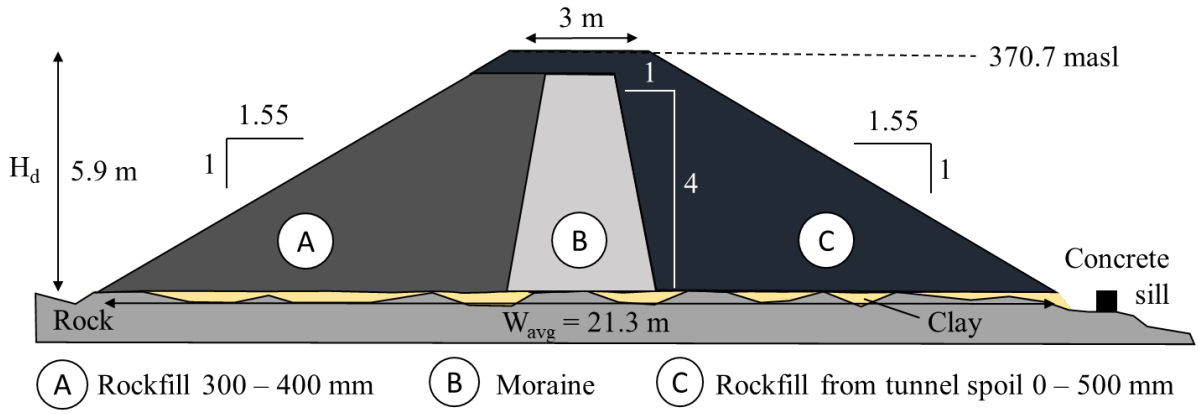

Figure 5. Test 1-2003, zoned rockfill with moraine core dam.

Table 6. Material properties of prototype dam T1-2003 (Morris, 2009).

	Moraine	Rockfill
Moisture content	0.06	0.02
D50 (mm)	7	85
Porosity	0.244	0.235
Friction angle	45.6	42
Grain density ($g.cm^{-3}$)	2.77	2.77
Cohesion ($kN.m^{-2}$)	20	/
Dry density ($kN.m^{-3}$)	20.6	/

3.1.4 Historical failure cases from the literature

To put into perspective the results from prototype dams on the experimental site, we also consider the use of breaching parametric equations for some historical failure cases taken from the literature. The main characteristics of these dams as well as references for readers eager to learn more about these cases are displayed in Table 7. Most of this information was directly extracted from Xu and Zhang (2009) and Froehlich (2016b).

Table 7. Historical dams' characteristics.

Dam name	Banqiao	Shimantan	Butler Valley	Oros	Cougar Creek
Country	China	China	USA	Brazil	Canada
Type	Earthfill, homogeneous	Earthfill, homogeneous	Earthfill, homogeneous	Earthfill, rockfill, zoned	Rockfill, homogeneous
Erodibility	High Erodibility	High Erodibility	/	Low erodibility	Medium erodibility
Year completed	1953	1953	/	1960	1982
Year failed	1975	1975	1982	1960	1990
References	Fujia and Yumei (1994), Qing (1998), Henan Water Resources Authority (2005), Courivaud (2007), Xu et al. (2009)	Fujia and Yumei (1994), Qing (1998), Xu et al. (2008)	Aldridge (1987)	ICOLD (1974), Jansen (1983)	McEwen (1991)

3.2 Data acquisition

By using the measured water elevation in the reservoir above the breach bottom (h_w), one can compute the volume of water when the failure starts (V_w) using the reservoir capacity curves (Figure 6). Similarly, the full reservoir capacity (S) can be estimated according to the dam height (h_d). This information is then used to obtain hydrographs (Figures 10, 14, and 18), which show the variation in water flow ($m^3.s^{-1}$) over time (s). The maximum amount of water released during the breaching event, known as the peak outflow value (Q_p), can be read off these hydrographs. However, because of the weather conditions for T2-2002, it must be highlighted that an ice jam was most likely present at VM5 (Figure 2), overestimating the water level and consequently the discharge values when using the rating curve. For this specific test, the outflow hydrograph calculated by HEC-RAS (EBL Kompetanse 2006), with the correct outflow volume will be used in this study.

The failure time (t_f) can also be estimated from the hydrographs. According to Morris et al. (2009), the failure time is the time between the start of the breach formation phase and the end of that phase. This corresponds to the time when the flow suddenly starts to rise until it comes back to a more stable value on the hydrograph. It is also at this point that the breach depth (h_b) and average breach width (B_{avg}) can be measured. The average width of the embankment above the breach bottom (W_{avg}) can also be measured at this time. The input parameters measured for each model, as well as the ones from historical failure cases, are used to compute the results of the parametric equation and are listed in Table 8.

To aid in monitoring the deformation and breach opening of the dam through time, a grid measuring 1 × 2 m was sprayed onto both the crest and downstream slope. Throughout the testing process, numerous digital video cameras were used for continuous recording. A grid was manually drawn on top of the picture using Adobe Photoshop and then imported to Adobe Premiere along with the actual video for rendering (more information available in EBL Kompetanse (2006)). A new video with a visible grid was created by stopping the video every 5 seconds to register any changes in the breach opening at the downstream dam face. The time and breach width at every 0.5 m vertically were recorded at each abrupt change in the breach opening. In the case of continuous erosion, the breach width was noted after an increase of about 0.5 m. A resolution of 0.5 m in the lateral direction was applied in most of

the tests, but a resolution of 0.1 m was possible in some tests, depending on the video quality and the conditions at the dam.

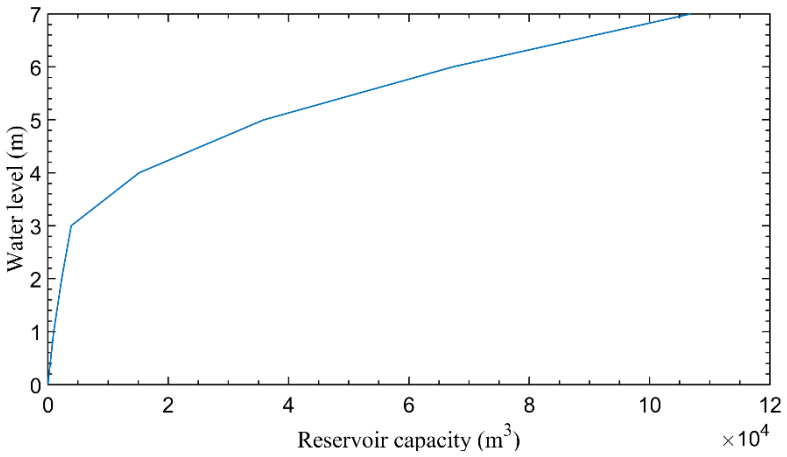

Figure 6. Reservoir capacity of prototype dams from the IMPACT project.

Table 8. Input parameter values used for parametric equations displayed in Tables 1-3, for each experimental model.

Dam name	Type	h_d (m)	h_b (m)	h_w (m)	W_{avg} (m)	V_w (m^3)	S (m^3)
T1-2002	Earthfill homogeneous	5.9	5.9	5.8	29.4	61 035	64 176
T2-2002	Rockfill homogeneous	5	5	5	19.5	35 901	35 901
T1-2003	Rockfill zoned	5.9	5.9	6.1	21.3	71 272	64 176
Banqiao	Earthfill homogeneous	24.5	29.5	31.9	97	701.10^6	492.10^6
Shimantan	Earthfill homogeneous	25	25.8	27.4	58	$167. 10^6$	$94.4.10^6$
Butler Valley	Earthfill homogeneous	/	7.16	7.16	9.63	$2.4.10^6$	/
Oros	Earthfill and rockfill zoned	35.4	35.5	35.8	110	660.10^6	650.10^6
Cougar creek	Rockfill homogeneous	10	10.4	11.1	21.7	29 800	/

3.3 Breach formation

The breaching parameters (B_{avg}, t_f, and Q_p) measured for each experimental dam (T1-2002, T2-2002, and T1-2003) and historical cases are displayed in Table 9. Unfortunately, no data is available in the literature concerning the breach formation time of Butler Valley dam. No

information on the final breach width and peak outflow could be encountered either for Cougar Creek dam. Different orders of magnitude can be observed for the different cases because of the very different dimensions of dams and reservoirs (Table 8). These values as well as the ability of the parametric equations to estimate them are detailed in the Discussion section.

From the video recordings of the failures of the prototype dams, we could plot the breach opening using the MATLAB plotting tool. The opening, considered in the center of the models, is displayed in 2 dimensions (breach width and breach depth) along with time for models T1-2002 (Figure 7), T2-2002 (Figure 11), and T1-2003 (Figure 15). Also, the breach width growth along with time is displayed for both downstream and central sections for models T1-2002 (Figure 9), T2-2002 (Figure 13), and T1-2003 (Figure 17). The hydrographs, displaying the water level upstream of the dam (VM2, Figure 2) and the outflow from the dam (from VM5 data for T1-2002 and T1-2003 and HEC-RAS for T2-2002 model) are finally presented in Figures 10, 14 and 18 and a comparison between all of them is displayed in Figure 19.

Table 9. Breaching parameters measured for each prototype dam and historical case.

Dam name	Type	Breach width, B_{avg} (m)	Breach formation time, t_f (hrs)	Peak outflow, Q_p (m^3/s)
T1-2002	Earthfill homogeneous	26.3	1.58	401
T2-2002	Rockfill homogeneous	10.6	0.13	75
T1-2003	Rockfill zoned	17	0.15	242
Banqiao	Earthfill homogeneous	291	5.5	56 300
Shimantan	Earthfill homogeneous	367	3	25 300
Butler Valley	Earthfill homogeneous	62.5	/	810
Oros	Earthfill and rockfill zoned	200	6.5	58 000
Cougar Creek	Rockfill homogeneous	/	0.083	/

3.3.1 T1-2002 dam

The homogeneous earthfill T1-2002 model underwent a discrete and long breaching process of the clayey material (Figure 10). The water reached the pilot channel at 11:15 and the failure started at 12:55 without any overtopping of the dam crest. The breaching mainly consisted of vertical erosion to the bottom of the structure (until 13:10) before observing an increase in the breach width (Figure 7). The comparison between the breach width in the center and in the downstream section (Figures 8 and 9) also conforms with that description. The final breach had almost vertical side walls. The maximum outflow occurred when the maximum breach width was reached (around 14:00, Figures 9 and 10). To keep the water level upstream, the water discharge from Røssvassdammen was decided to be increased continuously from 14 $m^3.s^{-1}$ at 13:08 to 396 $m^3.s^{-1}$ at 13:45 by opening two of the flood gates. The yellow water level curve displays that event in Figure 10.

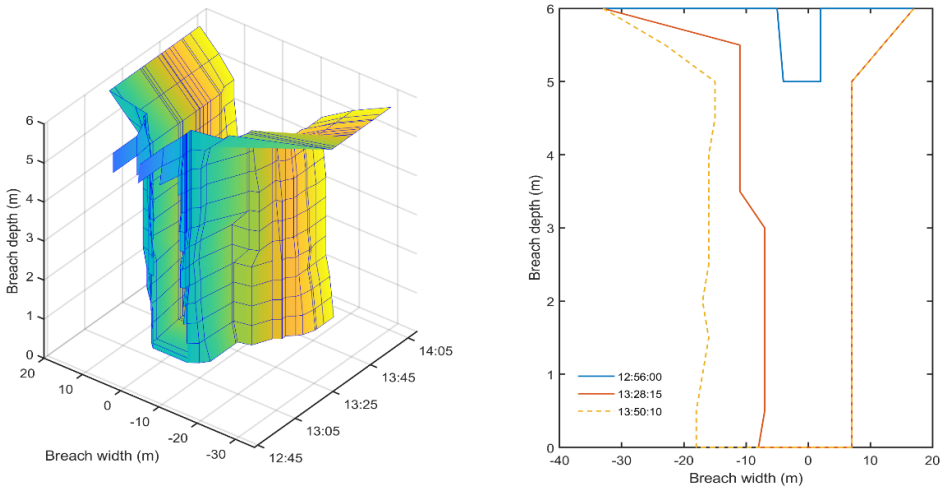

Figure 7. Breach width opening with time in the center of T1-2002 dam during failure.

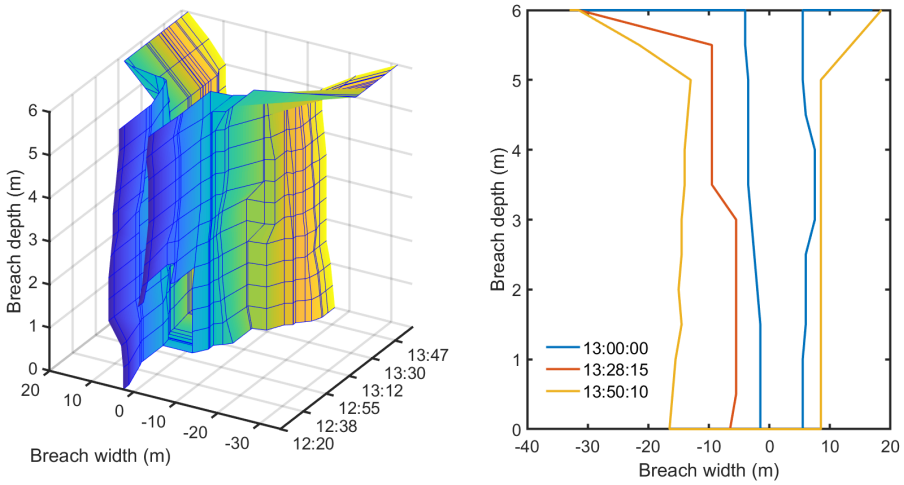

Figure 8. Breach width opening with time on the downstream face of T1-2002 dam during failure.

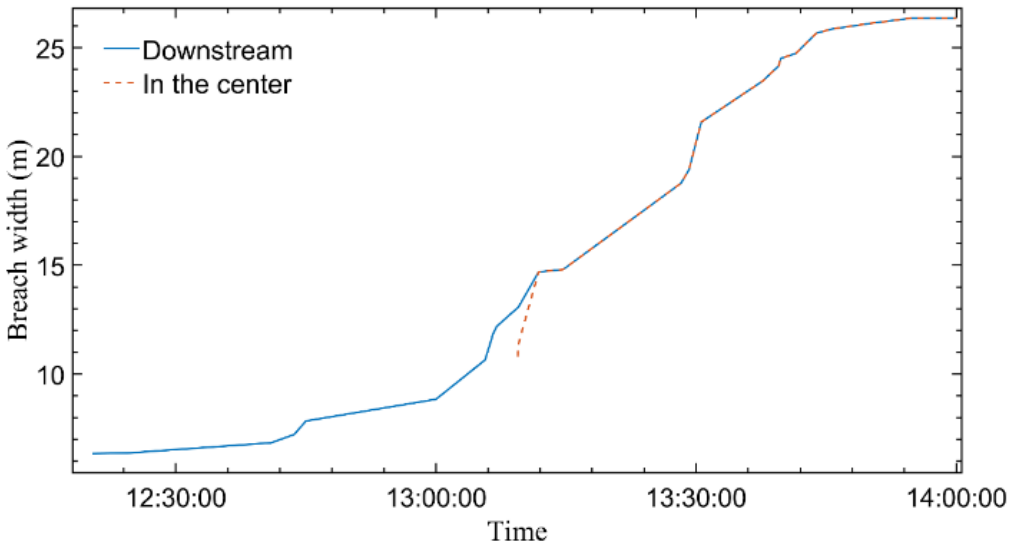

Figure 9. Average breach width in T1-2002 prototype dam during failure.

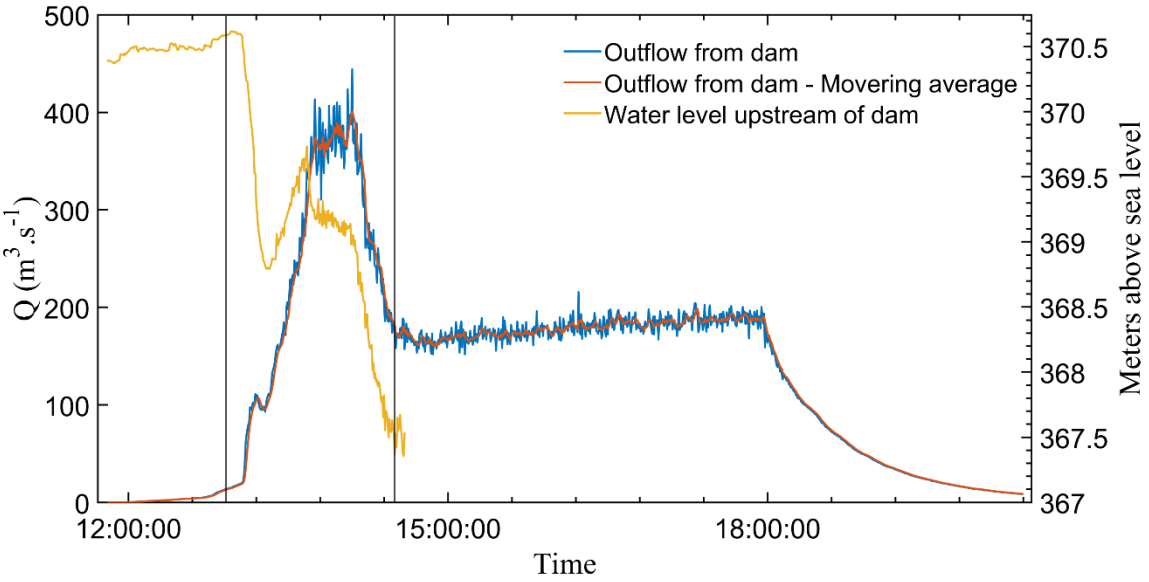

Figure 10. Stage (VM2) and flow (VM5) hydrographs for T1-2002 failure, adapted from EBL Kompetanse (2006). Vertical black lines stand for the beginning and the end of breach formation time.

3.3.2T2-2002 dam

The breach opening was much faster for the T2-2002 homogeneous rockfill dam (Figure 14) than it was for T1-2002. The erosion process was also more continuous with the slumping of materials of smaller volumes. The water reached the pilot channel at 11:42 (Figure 12) and the failure started at 12:22 without any overtopping of the dam crest. The erosion of the dam did not go through a first vertical incision to the bottom and then a widening of the breach as it did with the earthfill dam. The breaching was more progressive in both directions (Figure 11). Also, the breach width was more important in the downstream section than in the center (Figures 12 and 13). No additional flood gates were opened upstream during the breaching, with a constant release of water from the gates set to 1.2 $m^3.s^{-1}$, allowing the water level and outflow to decrease quite fast (Figure 14) and preventing Q_p and B_{avg} values to be as great as observed during the overtopping of T1-2002. The data considered for this hydrograph were directly computed using HEC-RAS (EBL Kompteanse, 2006), outlining the absence of noise on both curves.

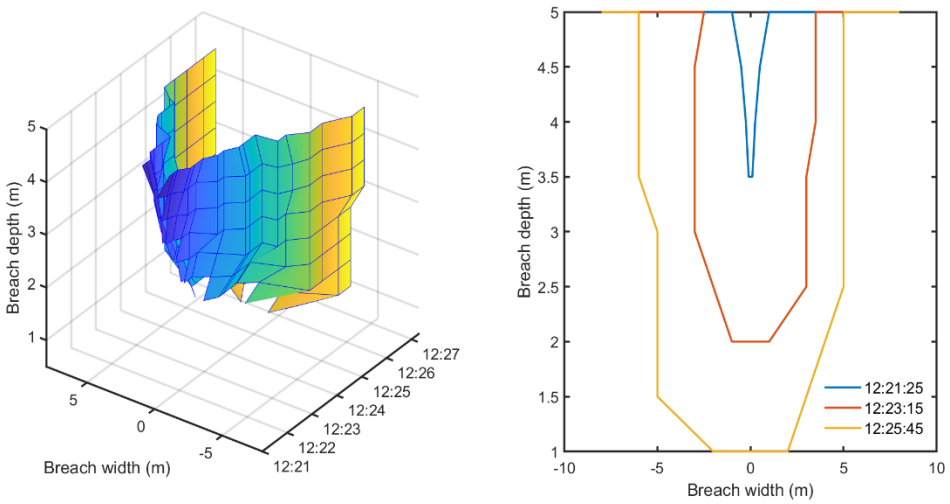

Figure 11. Breach width opening with time in the center of T2-2002 dam during failure.

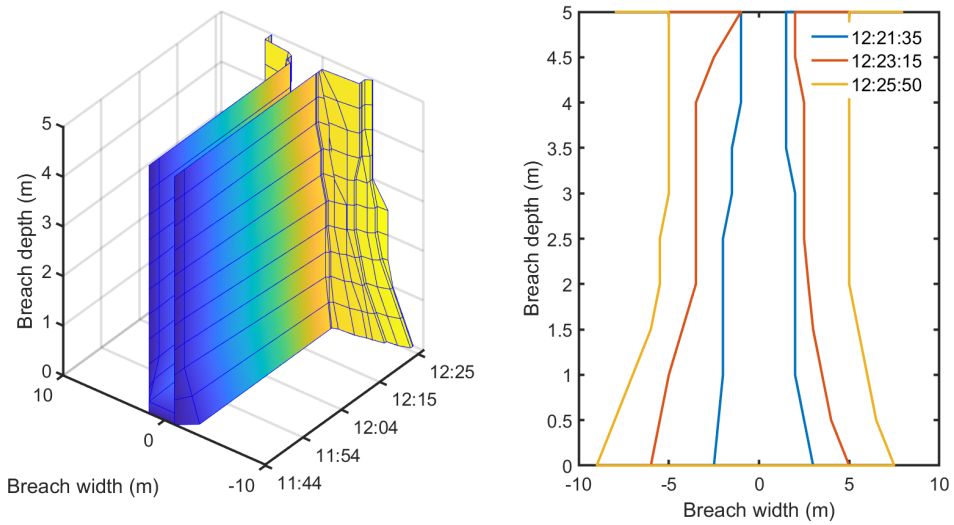

Figure 12. Breach width opening with time in the downstream face of T2-2002 dam during failure.

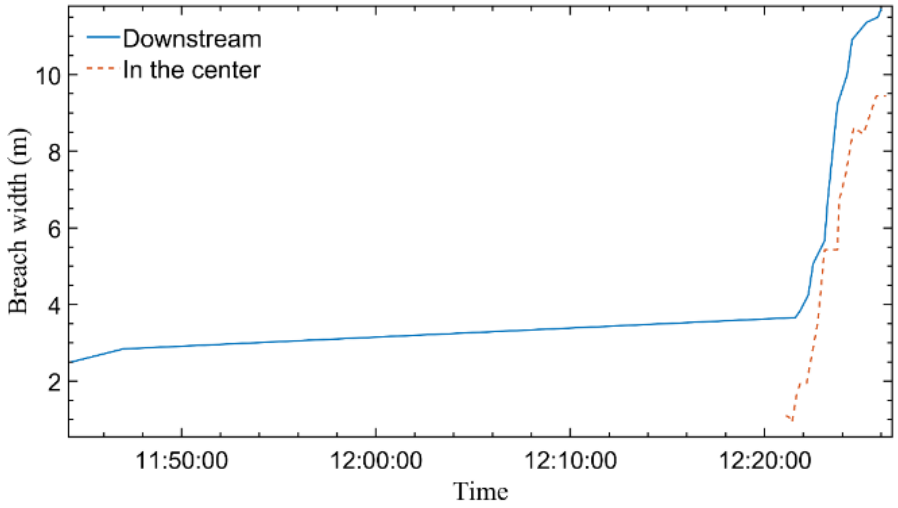

Figure 13. Average breach width in T2-2002 prototype dam during failure.

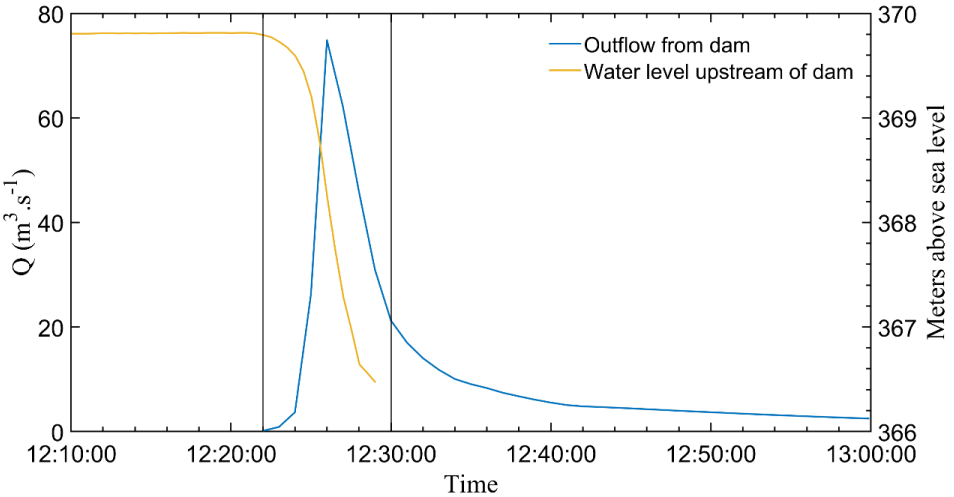

Figure 14. Stage (VM2) and flow (VM5) hydrographs for T2-2002 failure calculated by HEC-RAS, adapted from EBL Kompetanse (2006). Vertical black lines stand for the beginning and the end of breach formation time.

3.3.3T1-2003 dam

As for the other rockfill model T2-2002, the breaching of T1-2003 was fast (Figure 18). The water reached the pilot channel at 11:35 and the failure started at 13:55 with the overtopping of the dam crest starting at 12:40. The erosion process was quite irregular with large slumps of moraine from the dam core and smaller ones from the downstream fill. A clear difference in the erosion process from the core and the downstream fill can be observed in Figures 16 and 17. The breach width growth is more important in the gravel fill downstream but finally tends to be equal that the breach of the moraine core when the failure process ends. The central erosion appears to first occur vertically before widening and ending with almost vertical sides (Figure 15), as for T1-2002 model. The water level fell rapidly when the breaching started, the inflow from Røssvassdammen was 173 $m^3.s^{-1}$ and the floodgate was then closed at 14:09.

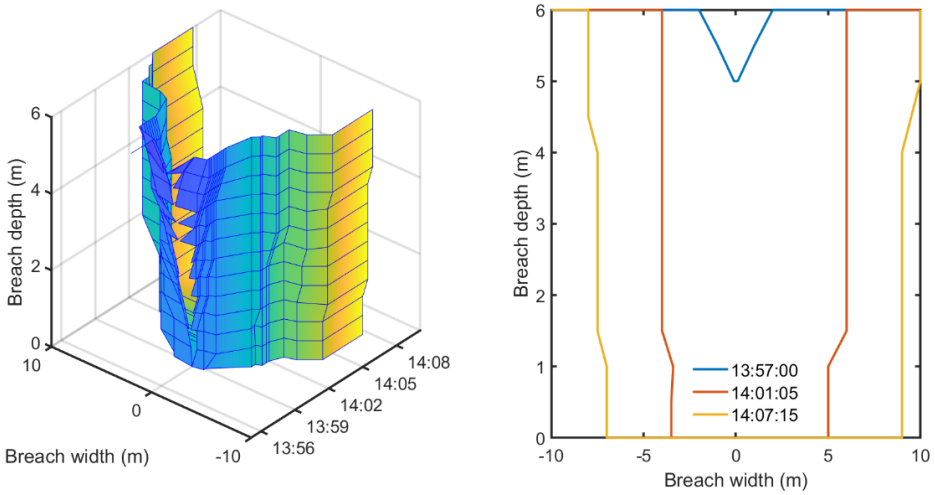

Figure 15. Breach width opening with time in the center of T1-2003 dam during failure.

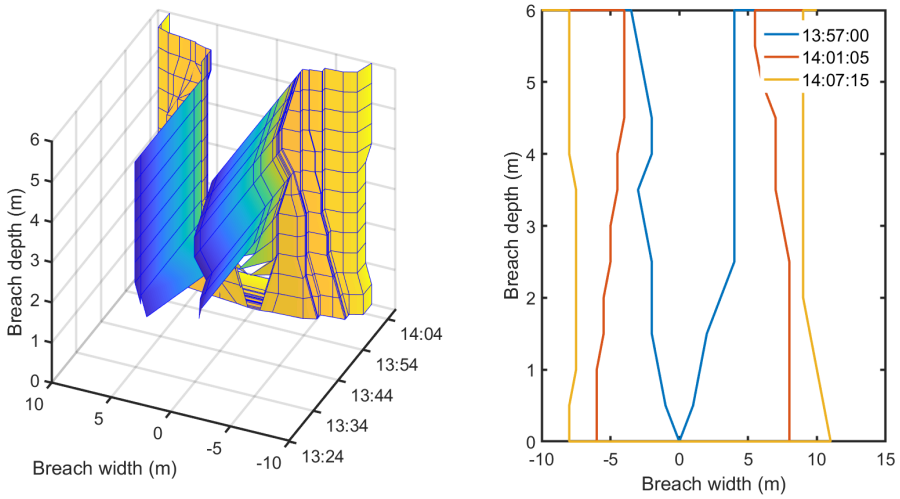

Figure 16. Breach width opening with time in the downstream face of T1-2003 dam during failure.

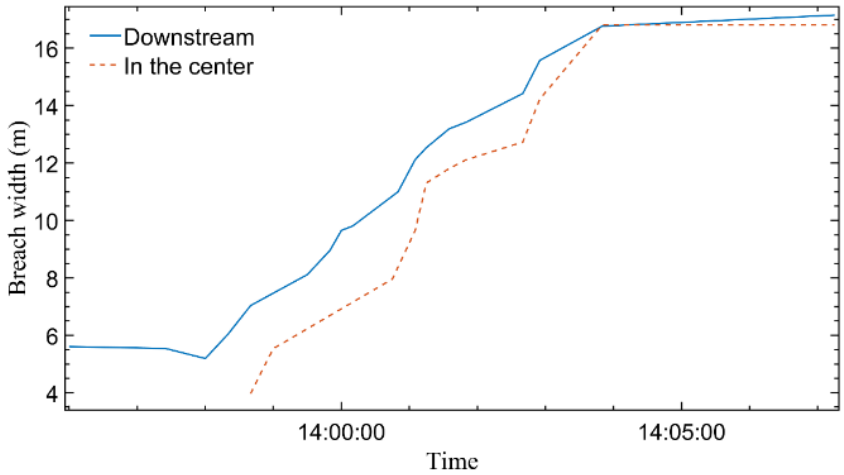

Figure 17. Average breach width in T1-2003 prototype dam during failure.

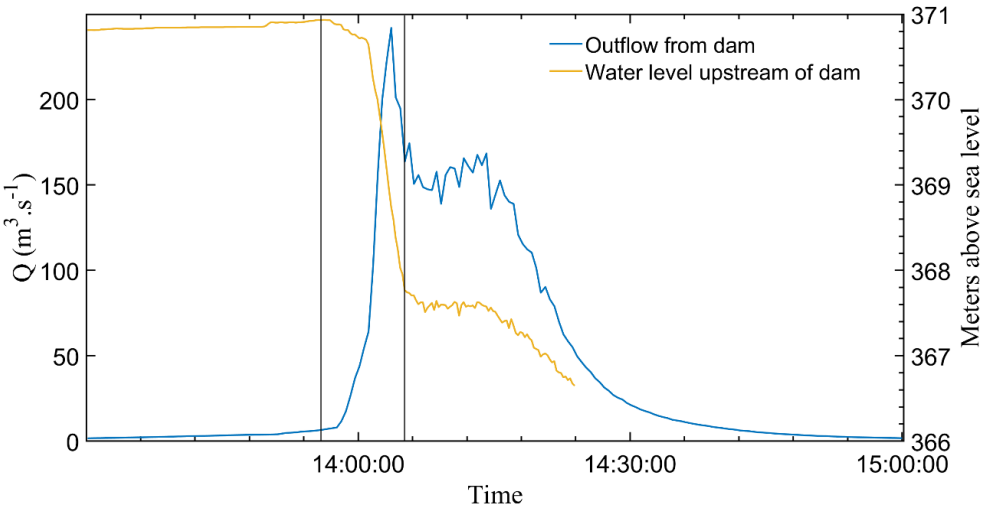

Figure 18. Stage (VM2) and flow (VM5) hydrographs for T1-2003 failure, adapted from EBL Kompetanse (2006). Vertical black lines stand for the beginning and the end of breach formation time.

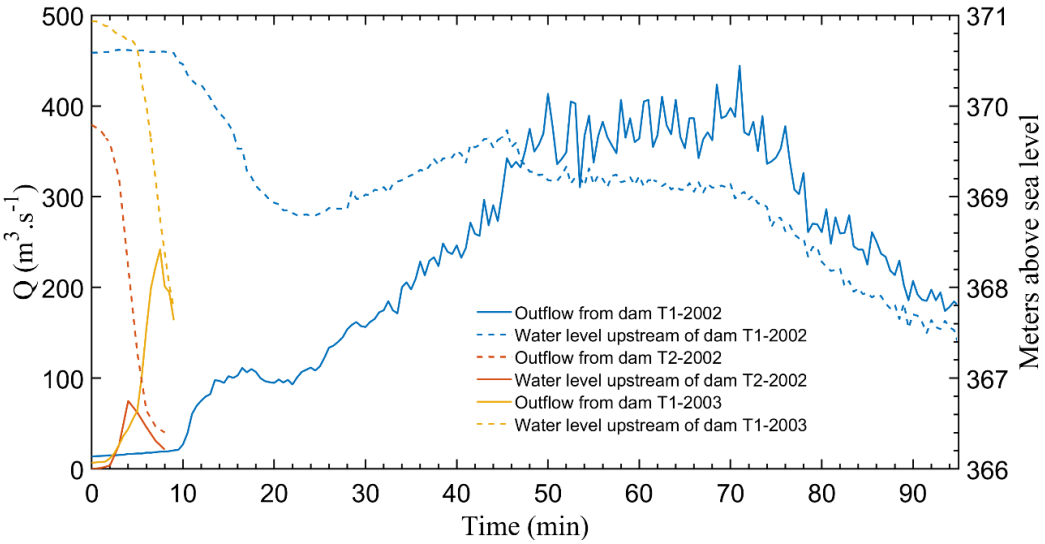

Figure 19. Stage (VM2) and flow (VM5) hydrographs for T1-2002, T2-2002, and T1-2003 failure from the beginning of breach formation.

3.4 Breaching parameters from parametric breach models

Using equations (1 - 31) and the input parameters (Table 8), the breaching parameters (B_{avg}, t_f, and Q_p) could be computed for all dams and are respectively displayed in Tables 10, 11, and 12 and discussed in the following section. We also display the Relative Root Mean Square Error (RRMSE) for each parametric model. In the tables, E, R, H, and Z provide information on the dam properties, respectively standing for embankment, rockfill, homogeneous, and zoned. Even though such analysis is not central in this research, Table 13 also displays the estimations obtained from the simplified physical breach models DLBreach for comparative appreciation (Wu 2016; Zhong et al. 2016). DLBreach is a model to predict the processes involved in the breaching of embankment dams. This model applies to both homogeneous dams with or without impervious cores, able to simulate two failure modes: overtopping and piping. DLBreach is grounded in the physical principles of hydraulics, sediment transportation, and soil mechanics, as well as the geometric and material properties of the embankment, and it considers the upstream boundary conditions. The DLBreach model generates various outputs, including the gradual growth of the embankment breach, the sediment transport rate, the elevation of the breach invert, the outflow hydrograph, and the widths of the breach's top and bottom.

Table 10. Breach width, B_{avg} (m), computed from equations displayed in Table 1 for all three models. The values in light grey and dark grey are respectively the ones contained in a ±30% and ±10% interval centered on the measured value (Table 9). ↓ and ↑ respectively stand for an underestimation and overestimation of the measured value.

Dam name	Measured breach width	U.S. Bureau of Reclamation (1988) Eq. 1	U.S. Bureau of Reclamation (1988) Eq. 2	Froehlich (1995a) Eq. 3	Froehlich (2008) Eq. 4	Xu & Zhang (2009) Eq. 5	Froehlich (2016a) Eq. 6
T1-2002 (EH)	26.3	↓ 17.4	↓ 14.5	↓ 12	↓ 12.8	↓ 17.67	↓ 13.6
T2-2002 (RH)	10.6	↑ 15	↑ 12.5	↓ 9.8	↑ 10.7	↓ 9.3	↑ 11.4
T1-2003 (RZ)	17	↑ 18.3	↓ 15.25	↓ 12.6	↓ 13.5	↓ 11.5	↓ 14.3
Banqiao (EH)	291	↓ 95.7	↓ 79.8	↑ 325.2	↓ 272.1	↓ 267.4	↑ 306.5
Shimantan (EH)	367	↓ 82.2	↓ 68.5	↓ 200.3	↓ 171	↓ 189.6	↓ 190
Butler Valley (EH)	62.5	↓ 21.5	↓ 17.9	↓ 40.3	↓ 41.7	/	↓ 46.1
Oros (ERZ)	200	↓ 107.4	↓ 89.5	↑ 330.4	↑ 268.9	↓ 156.4	↑ 300.4
RRMSE	/	13.96	14.93	8.38	8.15	7.73	7.96

Table 11. Breach formation time, t_f (hrs), computed from equations displayed in Table 2 for all three models. The values in light grey and dark grey are respectively the ones contained in a ±30% and ±10% interval centered on the measured value (Table 9). ↓ and ↑ respectively stand for an underestimation and overestimation of the measured value.

Dam name	Measured breach formation time	MacDonald & Langridge-Monopolis (1984) Eq. 7	MacDonald & Langridge-Monopolis (1984) Eq. 8	U.S. Bureau of Reclamation (1988) Eq. 9 Earthfill	U.S. Bureau of Reclamation (1988) Eq. 9 Rockfill	Froehlich (1995b) Eq. 10	Froehlich (2008) Eq. 11	Xu & Zhang (2009) Eq. 12	Froehlich (2016a) Eq. 13
T1-2002 (EH)	1.58	↓ 0.17	↓ 0.12	↓ 0.19	↓ 0.1	↓ 0.18	↓ 0.23	↓ 0.23	↓ 0.22
T2-2002 (RH)	0.13	↑ 0.14	↓ 0.1	↑ 0.165	↓ 0.09	↑ 0.15	↑ 0.21	↑ 0.37	↑ 0.2
T1-2003 (RZ)	0.15	↑ 0.18	↓ 0.13	↑ 0.2	↓ 0.1	↑ 0.19	↑ 0.25	↑ 0.44	↑ 0.24
Banqiao (EH)	5.5	↓ 3.75	↓ 3.7	↓ 1.05	↓ 0.55	↑ 5.88	↓ 5.03	↓ 3.56	↓ 4.78
Shimantan (EH)	3	↓ 2.4	↓ 2.26	↓ 0.9	↓ 0.47	↑ 3.1	↓ 2.81	↓ 2.42	↓ 2.67
Oros (ERZ)	6.5	↓ 3.8	↓ 3.76	↓ 1.18	↓ 0.61	↓ 4.82	↓ 4.06	↑ 23.25	↓ 3.85
Cougar Creek (RH)	0.08	↑ 0.17	↑ 0.12	↑ 0.37	↑ 0.19	↓ 0.07	↑ 0.09	↑ 0.21	↑ 0.09
RRMSE	/	7.95	8.18	16.48	18.37	4.96	6.33	37.78	6.88

Table 12. Peak outflow, Q_p (m^3/s), computed from equations displayed in Table 3 for all three models. The values in light grey and dark grey are respectively the ones contained in a ±30% and ±10% interval centered on the measured value (Table 9). ↓ and ↑ respectively stand for an underestimation and overestimation of the measured value.

Dam name	Measured peak outflow	Soil Conservation Service (1981) Eq. 14	Singh & Snorrason (1982) Eq. 15	Singh & Snorrason (1984) Eq. 16	MacDonald & Langridge-Monopolis (1984) Eq. 17	U.S. Bureau of Reclamation (1982) Eq. 18	Costa (1985) Eq. 19	Costa (1985) Eq. 20	Evans (1986) Eq. 21	Froehlich (1995b) Eq. 22
T1-2002 (EH)	401	↑ 429	↓ 384	↓ 323	↓ 223	↑ 494	↑ 599	↓ 212	↓ 248	↓ 139
T2-2002 (RH)	75	↑ 326	↑ 281	↑ 246	↑ 169	↑ 375	↑ 443	↑ 158	↑ 187	↑ 99
T1-2003 (RZ)	242	↑ 471	↑ 384	↑ 323	↑ 243	↑ 542	↑ 655	226	↑ 269	↓ 154
Butler Valley (EH)	810	↓ 633	/	/	↑ 1 100	↓ 729	↑ 4 838	/	↑ 1 726	↓ 530
Banqiao (EH)	56 300	↓ 10 049	↓ 5 658	↓ 21 611	↓ 21 194	↓ 11 562	↑ 123 610	↓ 19 513	↓ 35 121	↓ 18 087
Shimantan (EH)	25 300	↓ 7 585	↓ 5 878	↓ 9 947	↓ 11 023	↓ 8 727	↑ 54 658	↓ 10 773	↓ 16 420	↓ 9 811
Oros (ERZ)	58 000	↓ 12 439	↓ 11 343	↓ 24 633	↓ 21 680	↓ 14 313	↑ 119 435	↓ 22 205	↓ 34 017	↓ 20 501
RRMSE	/	18.02	20.7	14.61	14.06	17.33	25.66	15.43	8.9	14.93

Table 12 (continued). Peak outflow, Q_p (m^3/s), computed from equations displayed in Table 3 for all three models. The values in light grey and dark grey are respectively the ones contained in a ±30% and ±10% interval centered on the measured value (Table 9). ↓ and ↑ respectively stand for an underestimation and overestimation of the measured value.

Dam name	Measured peak outflow	Walder & O'Connor (1997) Eq. 23	Walder & O'Connor (1997) Eq. 24	Walder & O'Connor (1997) Eq. 25	Pierce (2008) Eq. 26	Pierce (2008) Eq. 27	Pierce (2008) Eq. 28	Pierce (2008) Eq. 29	Xu & Zhang (2009) Eq. 30	Froehlich (2016b) Eq. 31
T1-2002 (EH)	401	↓ 184	↓ 153	↓ 148	↓ 41	↓ 48	↓ 85	↓ 34	↓ 99	↓ 66
T2-2002 (RH)	75	↑ 144	↑ 108	↑ 111	↓ 27	↓ 32	↓ 57	↓ 23	↓ 44	↓ 49
T1-2003 (RZ)	242	↓ 198	↓ 172	↓ 162	↓ 46	↓ 55	↓ 98	↓ 38	↓ 78	↓ 85
Butler Valley (EH)	810	↑ 995	↓ 250	↓ 785	↓ 424	↓ 347	↓ 150	↓ 517	/	↑ 966
Banqiao (EH)	56 300	↓ 13 598	↓ 8 257	↓ 17 204	↓ 32 909	↓ 26 341	↓ 8 062	↓ 35 758	↓ 52 599	↓ 45 419
Shimantan (EH)	25 300	↓ 7 029	↓ 5 785	↓ 8 696	↓ 12 582	↓ 11 291	↓ 5 373	↓ 12 281	↓ 24 210	↓ 23 237
Oros (ERZ)	58 000	↓ 13 227	↓ 10 815	↓ 17 616	↓ 34 026	↓ 29 027	↓ 10 967	↓ 34 188	↓ 16 498	↓ 52 758
RRMSE	/	17.28	18.78	15.7	9.6	11.78	18.82	9.12	12.06	3.28

Table 13. Peak outflow, breach width, and failure time computed from the simplified physical breach model, DLBreach. The values in light grey and dark grey are respectively the ones contained in a ±30% and ±10% interval centered on the measured value (Table 9). ↓ and ↑ respectively stand for an underestimation and overestimation of the measured value.

Dam name	B_{avg} (m)		T_f (hrs)		Q_p ($m^3.s^{-1}$)	
	Measured	DLBreach	Measured	DLBreach	Measured	DLBreach
T1-2002 (EH)	26.3	↑ 27.25	1.58	↓ 1.32	401	↓ 399
T2-2002 (RH)	10.6	↑ 12.3	0.13	↑ 0.25	75	↑ 103
T1-2003 (RZ)	17	↓ 14.1	0.15	↑ 0.47	242	↓ 226

3.5 Discussion of the results

3.5.1 Suitability of breach width equations

The results obtained from breach width equations (Table 1) display the different abilities to describe the final breach width according to the dam example under concern (Table 10). First, it appears that no equation can provide a reasonable estimation (± 30% of the measured value) of the final breach width for all cases. Furthermore, no equation can describe reasonably B_{avg} for T1-2002 and Shimantan dams (both homogeneous earthfill dams).

Looking at the global ability of each equation to characterize all types of dams, Eq. 5 from Xu & Zhang (2009) appears to provide the best results with the lowest RRMSE value. The three equations (3, 4, and 6) from Froehlich (1995a, 2008, and 2016a) also display good RRMSE values (below 10%). However, the U.S. Bureau of Reclamation (1988) equations (Eqs. 1 and 2) have difficulty characterizing the breach widths, particularly the ones from higher dams (historical failure cases) where they always underestimate the measured values. This underestimation is especially problematic since these equations were meant to provide conservative results. These equations are only based on the use of h_w parameter and lack to be representative. Still, it is interesting to point out that Eq. (2), specifically dedicated to estimating B_{avg} for rockfill dams, could estimate well the breach values for both rockfill models with small h_w values (T2-2002 and T1-2003).

The volume of water when the failure starts (V_w) appears to be the most important parameter to be considered for B_{avg} estimation. Indeed, it is used in the four equations (Eq. 3-6) providing the best characterizations. Thus, the reservoir capacity has a central role in breach development. It also has to be highlighted that the breach widths of homogeneous earthfill dams are hard to estimate. While B_{avg} of Banqiao dam could be estimated pretty well with Eqs (3-6), B_{avg} values for the three other homogeneous earthfill dams (T1-2002, Shimantan, and Butler Valley) were all underestimated. Even though these cases all have different reservoir capacities. On the contrary, Froehlich equations (3, 4, and 6) tend to overestimate the breach width of the Oros dam. This probably comes from the fact that Oros dam has low erodibility material (Table 7). Xu & Zhang's (2009) equation (5) however can adapt to the properties of the material and provides a better estimation.

3.5.2 Suitability of failure time equations

As for the breach width equations, the failure time equations (Table 2) are not all able to characterize equally the duration of the breaching process (Table 11) according to the dam considered. However, one equation appears to behave better than the other introduced in this report. Indeed, Eq (10) from Froehlich (1995b) provides reasonable estimations for all cases, except for T1-2002 prototype dam, and has the lowest RRMSE value. Equations (7, 8, 11, and 13) from MacDonald & Langridge-Monopolis (1984), and Froehlich (2008 and 2016a) also present pretty good RRMSE values (below 10%). Contrary to the breach width characterization, Xu & Zhang (2009) Eq (12) is almost unable to characterize reasonably any of the failure times of the different cases. Eq (9) from the U.S. Bureau of Reclamation (1988) also provides a poor estimation of t_f.

The breach formation time measured for all cases seems to be directly correlated to the volume of water stored upstream of the dam. While Banqiao ($V_w = 701.10^6$), Shimantan ($V_w = 167.10^6$), and Oros ($V_w = 660.10^6$) dams took between 3 to 6.5 hours to fail, dams with smaller reservoirs such as T2-2002 ($V_w = 36.10^3$), T1-2003 ($V_w = 71.10^3$) and Cougar Creek ($V_w = 30.10^3$) failed much more rapidly, between 0.08 and 0.15 hours. Model T1-2002 is a particular case since the floodgates upstream were reopened during the overtopping process, bringing more water than what was initially stored in the reservoir. This certainly explains why all equations have difficulty estimating the failure time for this specific case. However, the number of cases in this study is not big enough to extract such a general

conclusion since the failure time can be affected by other variables not included in the parametric models. It is also of interest to notice that the dams displaying the fastest breaching process are the homogeneous and zoned rockfill dams (T2-2002, Cougar Creek, and T1-2003). Whereas, as we would have expected from structures made of more erodible materials, the dams containing earth took a longer time to reach the end of the breach formation phase.

Another interesting aspect to discuss is the overtopping time before the start of failure. The two homogeneous prototype dams (T1-2002 and T2-2002) did not undergo any proper overtopping of their crest. Only the overtopping of their pilot channel (respectively for 1.67 hours and 0.67 hours before the beginning of failure for T1-2002 and T2-2002) was required to breach them. However, the zoned model (T1-2003) displayed a higher level of resistance, undergoing an overtopping of the crest 1.25 hours before failure and even an overtopping of the pilot channel 2.33 hours before the beginning of failure.

While B_{avg} could not be estimated reasonably by the breach width equations for the failure of the Shimantan dam, the failure time is remarkably well estimated by almost all failure times equations, except Eq (9). All Froehlich equations (10, 11, and 13) provide good characterizations of t_f for the homogeneous earthfill or rockfill dams (Banqiao, Shimantan, and Cougar Creek). However, they overestimate t_f for small rockfill dams from the IMPACT project (T2-2002 and T1-2003). The results from MacDonald & Langridge-Monopolis (1984) equations (7 and 8) are difficult to discuss since no clear trend comes out from them. For example, Eq (7) for earthfill dams display a better ability to characterize t_f for rockfill structures than the one designed for non-earthfill dams. Some values tend to be underestimated in some cases and overestimated in others without clear justification.

3.5.3 Suitability of peak outflow

For the estimation of peak outflow (Q_p), there is a clear disparity between the equations able to characterize Q_p for smaller dams/reservoirs and the ones able to characterize the peak outflow for larger dimensions. No equation from Table 3 can estimate reasonably the measured peak outflow values (Table 12). Still, Eq (31) from Froehlich (2016b) appears to provide the best results, with the lowest RRMSE value. Eq (21) (Evans, 1986) and Eqs (26, 29) have also RRMSE values below 10% but none of them managed to estimate reasonably Q_p values for several historical cases or prototype dams.

As for the two previous breaching parameters investigated, the peak outflow is directly related to the dimensions of the dam and the reservoir. The order of magnitude can then be very different from one case to another. All historical cases' peak outflow could be well estimated using Eq (31) from Froehlich (2016b). Xu & Zhang (2009) also provides a good estimation of the volumes for historical homogeneous earthfill dams (Banqiao and Shimantan).

For smaller earthfill dams (T1-2002 and Butler Valley), the Soil Conservation Service (1981) equation (14), U.S. Bureau of Reclamation (1982) equation (18) and Singh and Snorasson (1984) equations (15, 16) based on earthfill dam rupture cases provide quite a good estimation. However, they underestimate dangerously the volumes for bigger structures (Banqiao, Shimantan, and Oros). For small zoned rockfill dam example we have (T1-2003), equations (17, 20, 21, 23, and 24) respectively from MacDonald & Langridge-Monopolis (1984), Costa (1985), Evans (1986) and Walder & O'Connor (1997) provide good estimation of Q_p.

3.5.4 Simplified physically based model

As expected, the estimations provided by DLBreach are quite close to the measured values. In particular, it is interesting to note the estimations obtained for the homogeneous earthen model (T1-2002) in Table 13. DLBreach provides the best estimations for this model, which aligns with the fact that DLBreach was developed for earthen embankment dams (Wu 2016). Where no equation was able to estimate the breach width and failure time for this model due to the inflow variation during testing, DLBreach offers very accurate estimations, mainly due to the consideration of upstream inflow values.

The estimations of breach widths (B_{avg}) and peak outflows (Q_p) are remarkably close to the measured values, regardless of the design or nature of the structure. However, the failure times (t_f) are overestimated for rockfill dams. Based on the obtained results, even though the simplified physically based model requires more data and computational resources, if possible, their usage is recommended due to their adaptability to different dam designs and inflow variations. Unfortunately, in the literature, required data on material properties, geometry of the embankment and inflow variations is missing for many of the historical cases that have been considered in this research work. Consequently, we cannot affirm that

the very good ability of the simplified physical model to estimate the breaching parameters is as effective for bigger dams.

3.5.5 Limitations

After discussing the results provided by the parametric equations for the estimation of B_{avg}, $t_{f,}$ and Q_p from historical cases and prototype dams from the IMPACT project, some limitations must be pointed out. First, of the three prototype dams, two underwent special events. Concerning dam T1-2002, flood gates upstream were opened during the breaching to try to keep the water level elevated (Figure 10). This action certainly enabled the breaching process to take a longer time (t_f), as well as to reach greater peak outflow (Q_p) and to provoke larger breach width (B_{avg}). This opening of the gates is certainly responsible for the bad characterization of the parameters from all the equations introduced in this report. Indeed, they are almost all underestimating the measured values (Tables 10 - 12). Concerning dam T2-2002, freezing occurred during the night, changing slightly the materials conditions. Indeed, as described in Morris (2009) there was extreme undercutting or overhanging of the crest material, indicating that the gravel was surely frozen at the surface level. The headcut development led to the point where the headcut broke through the upstream crest. The gravel embankment's clean, geometric cut-through headcut erosion during the breach test may be due to heavy compaction during construction, freezing conditions, or a combination of both factors. This suggests that freezing could have had a significant impact on flood conditions resulting from a breach. The headcut process is likely to have delayed breach formation and reduced the volume of water released before breach formation. As a result, the surge of water that occurred when breach formation eventually took place was more significant. Predictive models are expected to perform poorly against this test data as the one used in this report since none of them can simulate the effects of freezing.

Apart from these very specific dam conditions, when it comes to discussing the relevance of the parametric breaching equations, one must highlight the types of dams used to develop these equations. Indeed, there is a certain lack of representativity of rockfill dams in the literature. Many authors proposed relations focusing on earthen embankment dams (Soil Conservation Service 1981; Evans 1986; Froehlich 1995a, 2008, 2016a, 2016b; Pierce 2008; Xu & Zhang 2009) but only one reference focused on rockfill ones (U.S. Bureau of Reclamation 1988). Furthermore, the equations supposed to be representative of

embankment dams have been developed with a great majority of earthfill dams rather than rockfill ones. Besides the type of dam, our results point out that the design (either homogeneous or zoned dams) and the material properties are also of importance. For example, figures 11, 12, 15 and 16 display the difference between the breaching process and erosion mechanism according to the dam design. The settlement and extreme lateral erosion of T1-2002 (homogeneous earthfill) can also be observed in Figure 7. Unfortunately, Xu & Zhang (2009) is the only reference proposing the possibility to adapt the equations according to the specificity of the dam under concern. Our results also show that for the same type of dam, with a similar design, some equations can become more relevant than others according to the dimensions of the structure and its reservoir upstream. This suggests that new equations able to be adapted according to the type of dam, design, and dimensions should be developed to provide reasonable estimations.

Finally, the parametric breach models are not suited to take into consideration the dimensions of the pilot channels that were present in the prototype dams. Thus, we were unable to quantify to which extent this geometric specificity has affected the parametric breach model's estimations.

4 Laboratory experiments

This chapter is an adapted version of Dezert, Kiplesund and Sigtryggsdóttir(2024).

4.1 Experimental setup and methodology

The experimental models described in this chapter represent a full dam profile of a rockfill dam. These models are a development of earlier models used for investigating the stability of rockfill dams and ripraps under throughflow and overtopping situations. Instrumentation of the model includes pore pressure measurements along the dam foundation, water level recording and video recording from multiple angles as well as a detailed collection of imagery of the dam before and after testing. Still images and video recordings from several cameras are processed to develop detailed 3D models of the model before and after testing as well as developing dynamic 3D models of the dam model throughout the entire breaching process.

The model tests have been conducted in a flume at the Hydraulic Laboratory at the Norwegian University of Science and Technology (NTNU), Trondheim, Norway. The flume is horizontal with a length of 25 m, width of 1 m, and depth of 2 m (Figure 20). The maximum flow capacity of the flume is 0.5 m^3/s fed by three separate inlet pipes connected to a circulation system with an upper storage reservoir providing constant pressure. Inflow is measured using Siemens SITRANS FM Mag 5100 W sensors with Siemens SITRANS FM Mag 5000 transmitters with a flow rate measurement accuracy of ± 0.4 %. Upstream water levels are recorded with both a pressure sensor and an acoustic instrument. The pressure sensor is a SIEMENS SITRANS P210, 0 to 2450 mmWC. These sensors have a typical accuracy of 0.25 % (maximum 0.5 %) of the full-range value, which translates to ±6 mmWC for this sensor. The acoustic water level sensor is a Microsonic mic + 340 sensor with an accuracy of ±1 %. All sensors are connected to an Agilent U2355A device controlled by a computer; input voltage from each sensor is recorded at 100 Hz and stored on the computer. In addition to the data collection described above several video cameras were placed around the model to record the breach development as seen from the side as well as building dynamic 3D models seen from above using photogrammetric methods, as well as more

detailed 3D models being built before and after testing based on DSLR imagery, these methods are described in greater detail in Kiplesund et al (2023).

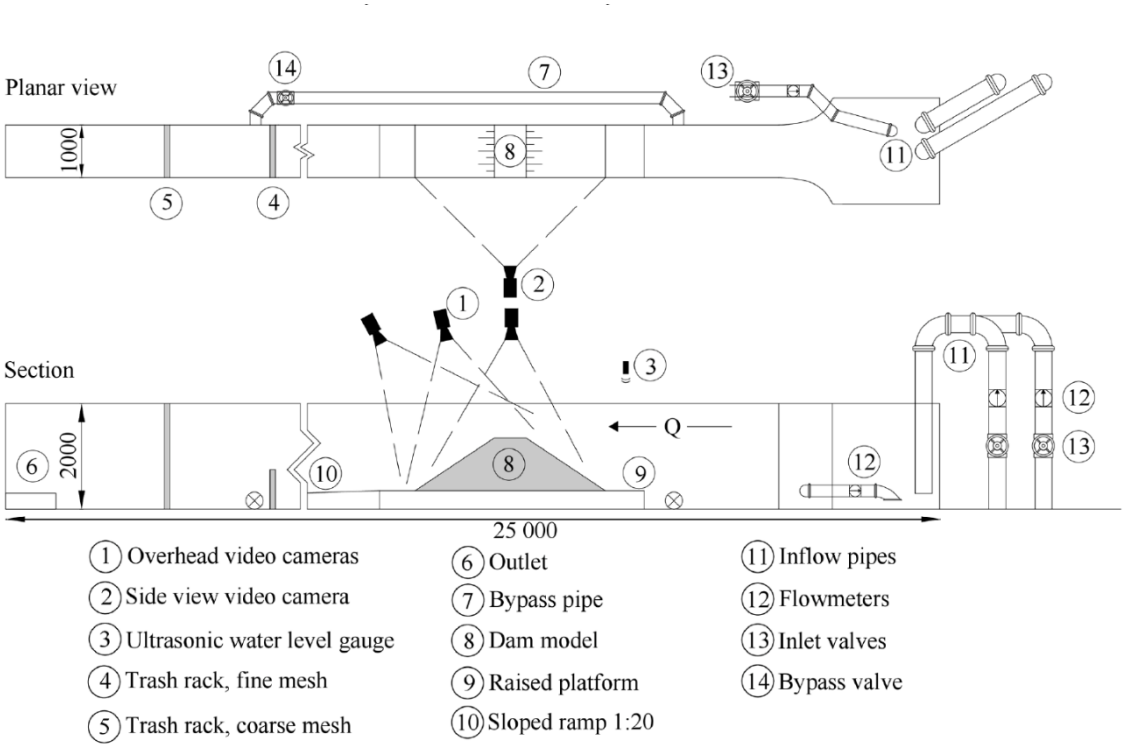

Figure 20. Hydraulic flume at NTNU (units in mm) from Kiplesund et al. (2023).

In this report chapter three different laboratory dam models are described: a model without any surface protection, a model with dumped riprap protection, and a model with placed riprap protection (Figure 21). The dam model without protection has a height of 1 m, a crest width of 0.6 m, slopes are 1:1.5 on both the upstream and downstream faces. The models are conceptual models of typical steep-sloped rockfill dams in 1:10 scale assuming Froude similarity where geometric dimensions and material sizes are scaled accordingly. The dam shoulder is comprised of well-graded rockfill material of density $\rho_{Shoulder}$ = 2720 kg·m^{-3}, median particle size d_{50} = 0.0065 m and a coefficient of uniformity $C_u = d_{60} \cdot d_{10}^{-1}$ = 7.7, the choice of material dimensions was based on measured gradation of existing dams as described in Kiplesund et al. (2023). Material smaller than 0.0005 m was sieved out of the shoulder material to prevent excessive amounts of fine material from entering the circulation system. For the riprap-protected dams, a uniformly graded filter layer of 0.1 m thickness, filter material density of ρ_{Filter} = 3050 kg·m^{-3} and d_{50} = 0.022 m, and a riprap layer of approximately 0.1 m are added. The riprap stone density is ρ_{Riprap} = 2600 kg·m^{-3} with d_{50} = 0.057 m and a C_u = 1.12, the diameter used here is an equivalent diameter calculated as $(a \cdot b \cdot c)^{1/3}$, where a, b, and c are the longest, middle and shortest axis respectively. Axis

lengths were measured for 550 rocks, density was measured for 50 of these. The rocks are angular with an average $a \cdot b^{-1}$=1.6. Dimensions of riprap and filter are based on Norwegian dam safety regulations in NVE (2012), a more detailed description of the choice of materials can be found in Ravindra et al. (2020). To reduce erosion of the downstream supporting fill and to ensure a realistic development of pore pressure in the supporting fill most of the models were built with a central impermeable core. One of the tests described here (Model H1) did not have an impermeable core, one test (Model CT2) used 0.1 x 0.05 m XPS foam rectangles with a sealing of PE film, the remaining models were constructed using a central core wall of 1 mm-thick styrene butadiene rubber (SBR 1729) with fiber reinforcement. Further details can be found in Kiplesund et al. (2023).

The dam models are placed on a 0.35 m high, 1 m wide, and 5 m long platform which is placed along a 4 m long section of glass wall in the upper part of the flume allowing for visual observation of the breach. The purpose of the platform and ramp is to secure a controlled downstream condition. Downstream of the platform is a 7 m-long ramp with a slope of 1V:20H. A horizontal pilot channel with varying dimensions was constructed on the crest towards the glass wall on some of the models. The purpose of the pilot channel is to ensure that the breach initiates along the glass wall to facilitate observation from outside the flume, enabling video recording from the side of the breach development in addition to the observation from above. For the subsequent analyses the breach is assumed perfectly symmetrical around the wall, this is a simplification of the real flow conditions in such a breach opening but is considered acceptable for the purposes of these analyses. Additional information for each model is displayed in Table 14.

Table 14. Overview of experimental models.

Model number	Core walls material	Leakage Flow (l/s)	No. Of Cameras Total	Pilot channel (bottom width, top width, depth in m)	Comments	Initial inflow (l/s)	Inflow increment	Inflow during breach (l/s)
Unprotected models								
CT2	XPS foam rectangles	1.3	6	0.1, 0.2, 0.1	/	5	/	8
U1	Rubber	1.0	6	0.1, 0.2, 0.1	/	5	/	5.5
U2	Rubber	0.7	6	0.1, 0.2, 0.1	/	5	/	5
U3	Rubber	0.7	6	0.1, 0.2, 0.1	/	10	/	10
U4	Rubber	0.2	6	0.1, 0.2, 0.1	/	5	/	5
U5	Rubber	0.3	9	0.1, 0.2, 0.1	/	15	/	15
H1	None	NA	9	0.1, 0.2, 0.1	/	15	/	15
Models with placed riprap								
P1	Rubber	0.2	6	0.1, 0.2, 0.1	/	5	5	50
P2	Rubber	0.4	6	0.3, 0.4, 0.1	/	5	5	40
P3	Rubber	0.2	6	/	/	5	5	55
P4	Rubber	0.3	9	/	No fiber cloth at the toe	5	5	25
Models with dumped riprap								
D1	Rubber	0.3	6	/	/	5	5	30
D3	Rubber	0.3	6	0.3, 0.4, 0.1	/	5	5	20
D4	Rubber	1.5	9	/	Thin layer of riprap	5	5	20

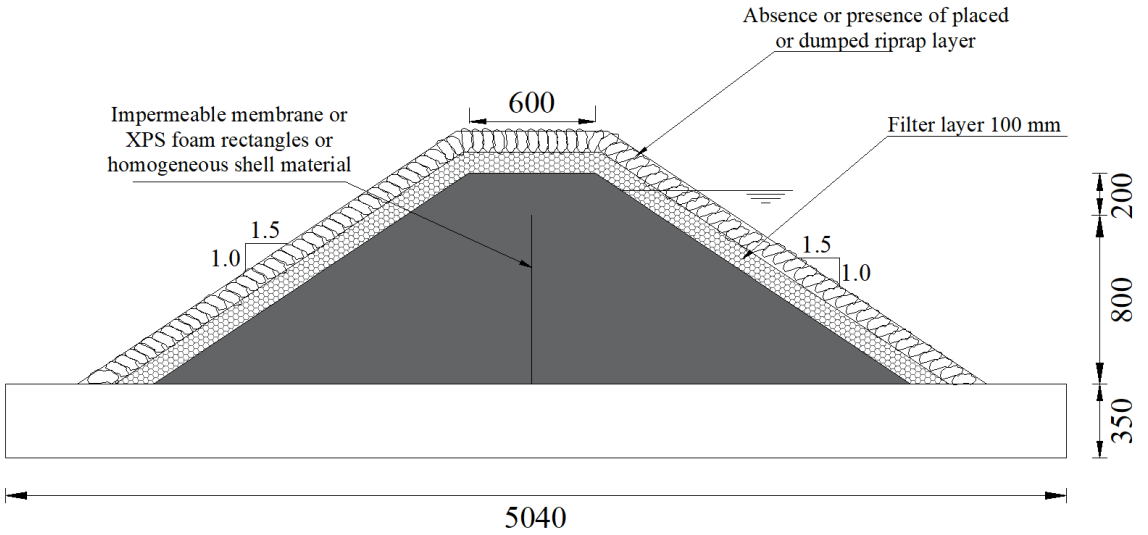

Figure 21. Geometry of experimental dam models.

The testing procedure was different for the protected and unprotected dams, the unprotected dams were tested by setting inflow at a specified target inflow shown in Table 14 as initial inflow, this inflow was kept constant as the core and crest overtopped and the dam failed. Inflow was closed after breach bottom erosion had stopped or was reduced to a low level as was the case for the high initial inflow tests where the initial inflow was sufficient to maintain some erosion for a long time. For dams with a core a leakage flow measurement was performed at a level just below the top of the impermeable core, this measured leakage flow is also shown in Table 14. The protected dams were tested by gradually ramping up inflow to the flume by 5 l/s every 30 minutes from an initial inflow of 5 l/s, this was continued until the dam breached. Inflow was stopped after breach bottom erosion had reduced to a low level or stopped completely. An example of water level and inflow variations for models D3, P3, and U3 is displayed in Figure 23.

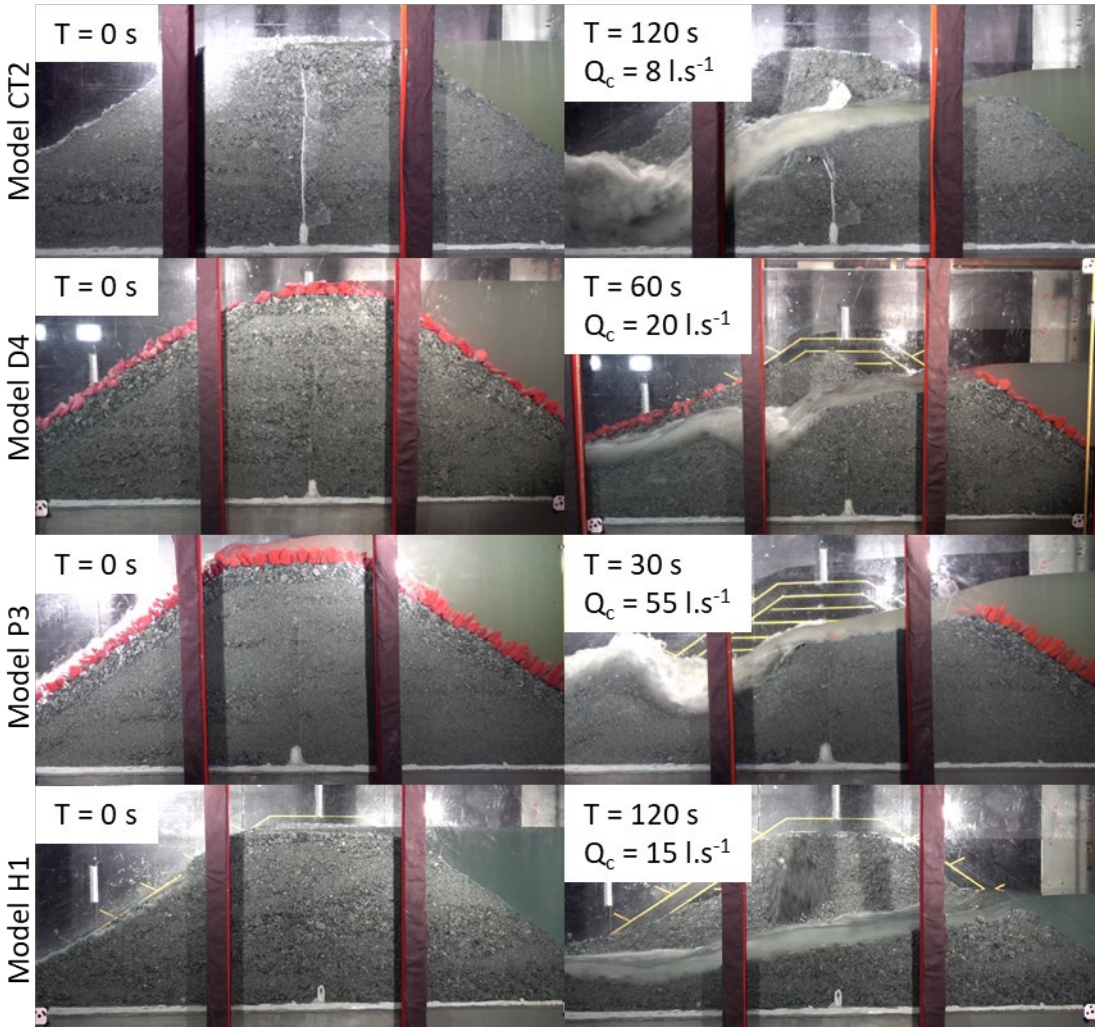

Figure 22. Pictures of dam failures for 4 types of dam designs used in this research.

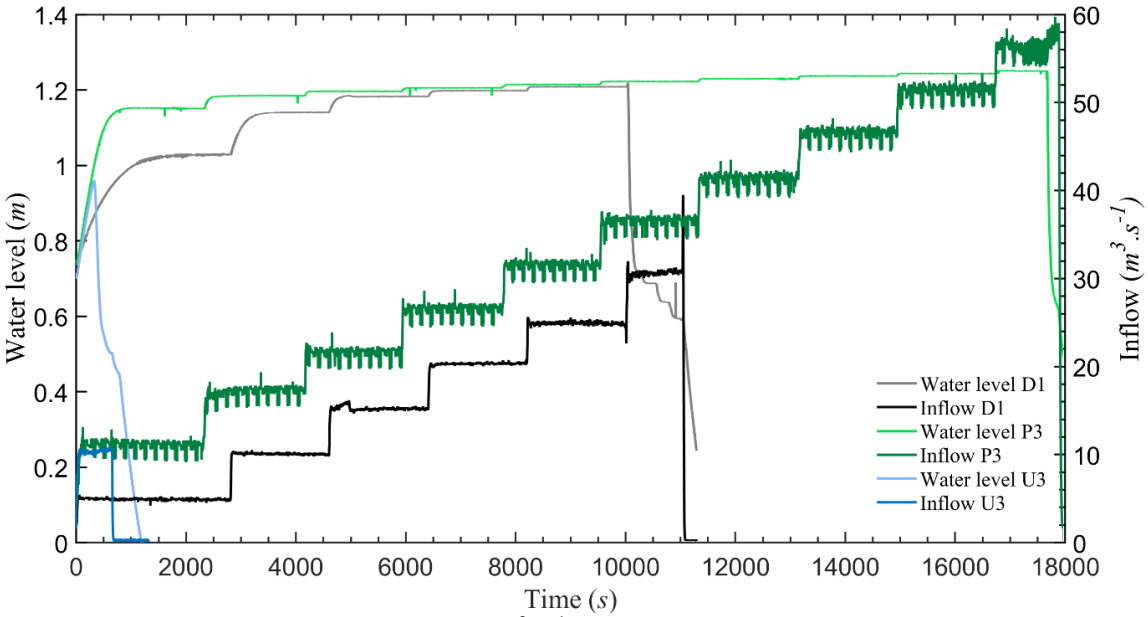

Figure 23. Water level (m) and inflow ($m^3.s^{-1}$) variations until failure for a dumped riprap model (D1), a placed riprap model (P3), and an unprotected model (U3).

4.2 Data acquisition

Using the measured water elevation in the reservoir above the breach bottom (h_w), the volume of water at the time of failure (V_w) can be computed thanks to the reservoir capacity curves for both protected and unprotected models. The full reservoir capacity (S) is also estimated thanks to these capacity curves according to the dam height (h_d). The hydrographs (Figures 24 and 25) displaying the water flow variation ($l \cdot s^{-1}$) along with time (s) are then obtained. The peak outflow value (Q_p) is the maximum amount of water released during the breaching event and can thus be read on these hydrographs. However, since we consider our experimental models to be representing a dam twice as wide (2 m wide instead of 1 m wide), the measured volume of water (V_w), reservoir capacity (S), peak outflow (Q_p), and breach width (B_{avg}) values need to be doubled to use and compare the parametric breaching equations results.

From such a hydrograph, the failure time (t_f), can also be estimated. According to Morris et al. (2009), the failure time corresponds to the time needed between the beginning of the breach formation phase and the end of that breach formation. This corresponds, on the hydrograph, to the time when the flow suddenly starts to rise until the moment when the flow comes back to a more stabilized value. It is also precisely when the breach formation ends that the breach depth (h_b) and average breach width (B_{avg}) can be measured from the 3D models of the dams, at the center of the crest, for $x = 0$ m. This is also at that time that the average width of the embankment above the breach bottom (W_{avg}) can be measured. The input parameters measured for each model and used for computing the parametric equation's results are displayed in Table 15.

Geometric data on breach development has been derived in two main ways, digitalization of breach bottom elevations as observed from the side seen through the glass wall and 3D models developed by way of photogrammetry, static models were developed from SLR photography taken before and after testing and dynamic models were developed using synchronized images extracted from video recordings from multiple angles above the models. Dynamic 3D models were only prepared for the tests without riprap since the riprap tests failed at a discharge where the model was completely covered by water and very limited data could be derived by photogrammetry, furthermore, the breaches of riprap protected dams were quite 2-dimensional in behavior and the dynamic 3D models could offer little

additional data beyond what could be derived from the side view analysis. The process of side-view analysis and photogrammetric model development is described in far more detail in Kiplesund et al. (2023).

Table 15. Input parameter values used for parametric equations displayed in Tables 1-3, for each experimental model.

Model number	h_d (m)	h_b (m)	h_w (m)	W_{avg} (m)	V_w (m^3)	S (m^3)
Unprotected models						
CT2	1	0.68	0.65	2.64	12.45	19.53
U1	1	0.67	0.61	2.61	11.66	19.53
U2	1	0.66	0.61	2.58	11.66	19.53
U3	1	0.67	0.63	2.61	12.05	19.53
U4	1	0.67	0.63	2.61	12.05	19.53
U5	1	0.63	0.61	2.49	11.28	19.53
H1	1	0.68	0.66	2.64	12.65	19.53
Models with placed riprap						
P1	1.2	0.67	0.71	2.01	13.30	23.05
P2	1.17	0.64	0.66	2.01	12.32	22.45
P3	1.18	0.58	0.65	1.8	12.13	22.45
P4	1.2	0.5	0.47	1.5	8.74	23.05
Models with dumped riprap						
D1	1.2	0.6	0.62	1.8	11.45	23.05
D3	1.2	0.44	0.44	1.32	8.11	23.05
D4	1.17	0.69	0.71	2.16	13.30	22.65

4.3 Breach formation

The failure mechanisms undergone by our models can be described as a surface erosion mechanism for unprotected and dumped riprap models, and as a sliding phenomenon for placed riprap models. The unprotected models underwent progressive surface erosion for very small overtopping discharges. Similarly, for dumped riprap, the flow forces progressively eroded the individual riprap stones, which resisted through their self-weight and frictional forces with the coarse filter layer. The failure occurred when the hydrodynamic forces surpassed the resultant of these two components. For the placed riprap models, as described in Dezert et al. (2022), the hydraulic drag and lift forces caused a rearrangement of the stones in the riprap layer, leading to their compaction and increased stability during the first overtopping event. As the discharge increases, some of the destabilizing forces are transferred to the filter layer and riprap toe built on the platform. When the hydrodynamic forces exceeded the static frictional forces, the entire placed riprap layer underwent a sliding mechanism.

Table 16 displays the breaching parameter values estimated for the 14 experimental models. The evolution of breach width, breach bottom elevation, water level, and outflow discharge are also plotted against time for both unprotected (Figure 24) and protected models (Figure 25). It appears that the peak outflow value for the dumped riprap models is almost twice as high as that of the unprotected models, while the placed riprap models show even more resistance, with a peak outflow value almost four times greater than that of the unprotected models. Due to the lack of fiber cloth of model P4, the peak outflow is closer to the ones observed for dumped models than for the other placed ones. However, the breach formation time is between 2 to 3 times more important for unprotected models than that of protected models (except for model D4 which has a thinner layer of dumped riprap, Table 14). It should be noted that the breach width could not be measured for protected models as the entire width of the dam was washed out during the breaching.

Table 16. Breaching parameters measured for each experimental model.

Model number	Breach width, B_{avg} (m)	Breach formation time, t_f (hrs)	Peak outflow, Q_p (m^3/s)
Unprotected models			
CT2	/	0.05	0.141
U1	0.92	0.05	0.112
U2	1.22	0.05	0.122
U3	1.4	0.044	0.112
U4	1.16	0.042	0.122
U5	1.22	0.047	0.148
H1	1.4	0.044	0.161
Models with placed riprap			
P1	/	0.025	0.389
P2	/	0.022	0.387
P3	/	0.014	0.459
P4	/	0.025	0.241
Models with dumped riprap			
D1	/	0.019	0.277
D3	/	0.022	0.238
D4	/	0.042	0.202

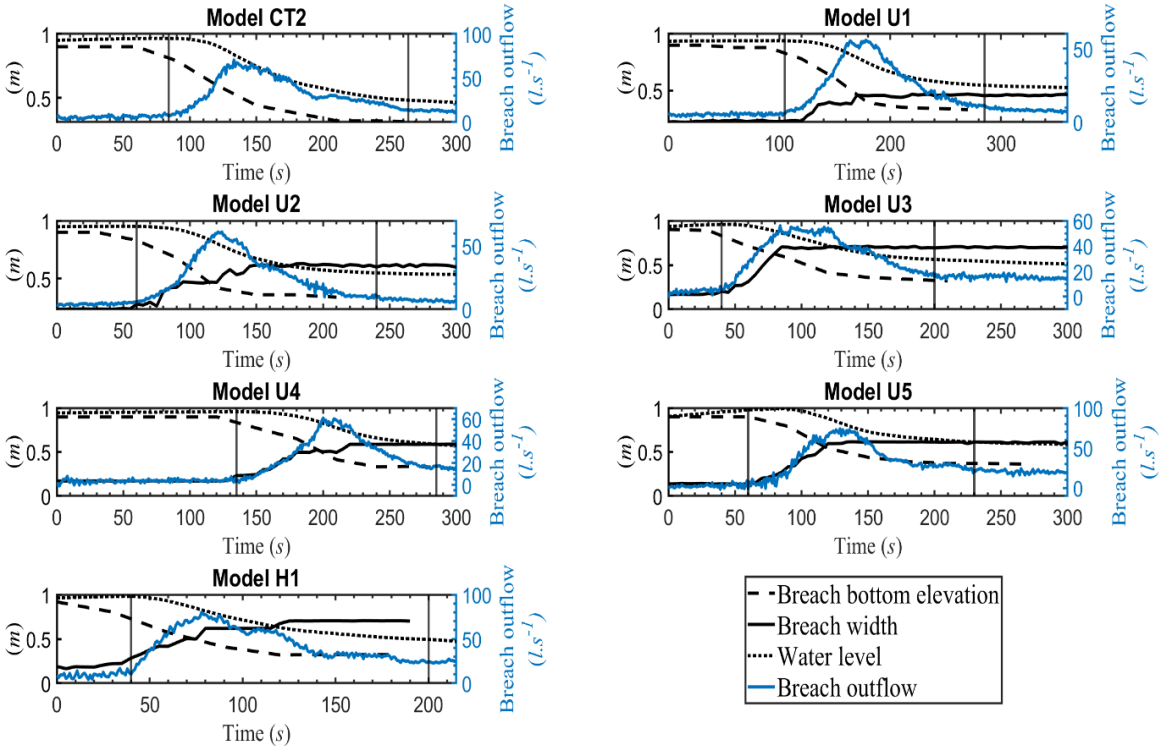

Figure 24. Breach width (m), breach bottom elevation (m), water level (m), and outflow discharge ($l.s^{-1}$) for unprotected models. The vertical dark lines stand for the beginning and end of failure time (s).

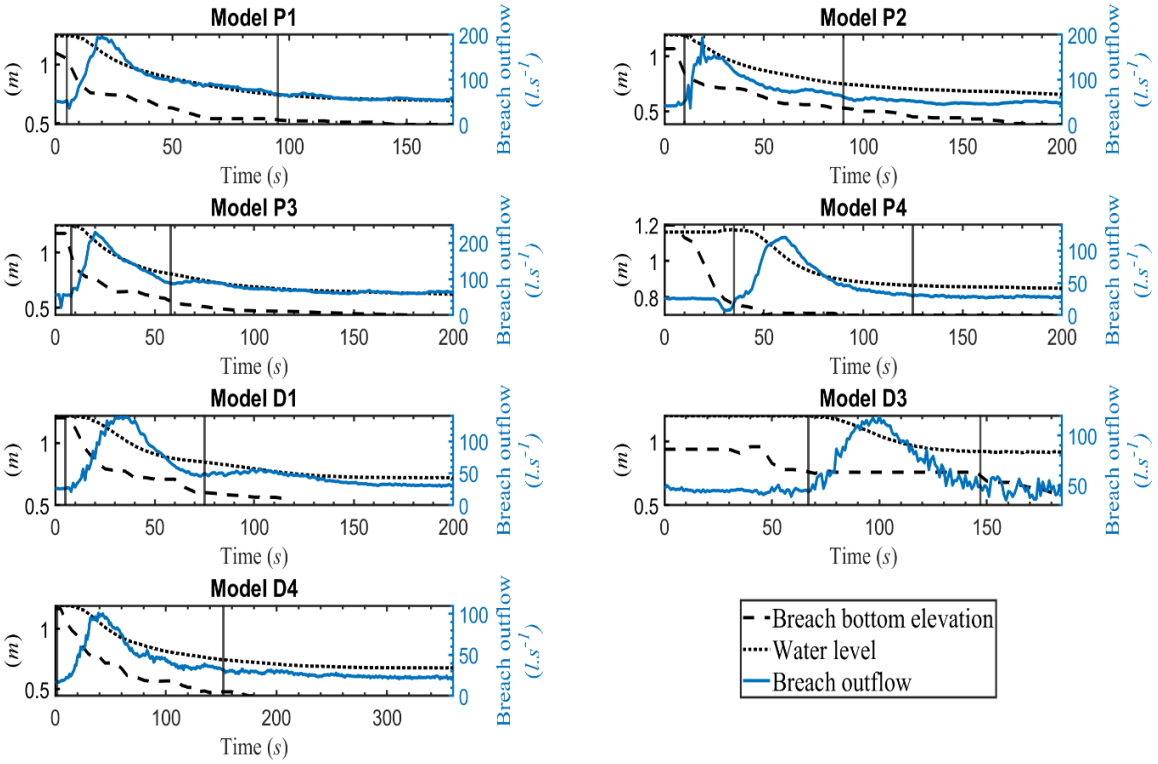

Figure 25. Breach width (m), breach bottom elevation (m), water level (m), and outflow discharge ($l.s^{-1}$) for protected models (dumped and placed riprap). The vertical dark lines stand for the beginning and end of failure time (s).

4.4 Breaching parameters from parametric breach models

From the input parameters (Table 15) and thanks to Eq. (1-31), the breaching parameters (B_{avg}, $t_{f,}$ and Q_p) could be computed for all 14 models. They are displayed in Tables 1-3 and discussed in the following section.

Table 17. Breach width, B_{avg} (m), computed from equations displayed in Table 1 for unprotected models. The values in light grey and dark grey are respectively the ones contained in a ±30% and ±10% interval centered on the measured value (Table 16). ↓ and ↑ respectively stand for an underestimation and overestimation of the measured value.

Model number	Measured breach width	U.S. Bureau of Reclamation (1988) Eq. 1 Earthfill	U.S. Bureau of Reclamation (1988) Eq. 2 Rockfill	Froehlich (1995a) Eq. 3	Froehlich (2008) Eq. 4	Xu & Zhang (2009) Eq. 5	Froehlich (2016a) Eq. 6
Unprotected models							
U1	0.92	↑ 1.83	↑ 1.52	↓ 0.51	↓ 0.76	↓ 0.84	↓ 0.78
U2	1.22	↑ 1.83	↑ 1.525	↓ 0.51	↓ 0.76	↓ 0.83	↓ 0.78
U3	1.4	↑ 1.88	↑ 1.57	↓ 0.52	↓ 0.77	↓ 0.83	↓ 0.79
U4	1.16	↑ 1.89	↑ 1.575	↓ 0.52	↓ 0.77	↓ 0.83	↓ 0.79
U5	1.22	↑ 1.82	↑ 1.515	↓ 0.5	↓ 0.75	↓ 0.79	↓ 0.77
H1	1.4	↑ 1.98	↑ 1.65	↓ 0.53	↓ 0.78	↓ 0.68	↓ 0.8
RRMSE	/	9.1	5	9.87	6.58	6.35	6.32

Table 18. Breach formation time, t_f (hrs), computed from equations displayed in Table 2 for all three models. The values in light grey and dark grey are respectively the ones contained in a ±30% and ±10% interval centered on the measured value (Table 16). ↓ and ↑ respectively stand for an underestimation and overestimation of the measured value.

Model number	Measured breach formation time	MacDonald & Langridge-Monopolis (1984) Eq. 7	MacDonald & Langridge-Monopolis (1984) Eq. 8	U.S. Bureau of Reclamation (1988) Eq. 9 Earthfill	U.S. Bureau of Reclamation (1988) Eq. 9 Rockfill
Unprotected models					
CT2	0.05	↓ 0.0085	↓ 0.00436	↓ 0.0133	↓ 0.0111
U1	0.05	↓ 0.0082	↓ 0.0042	↓ 0.0125	↓ 0.0104
U2	0.05	↓ 0.0082	↓ 0.0042	↓ 0.0125	↓ 0.0104
U3	0.044	↓ 0.0084	↓ 0.0043	↓ 0.0129	↓ 0.0107
U4	0.042	↓ 0.0084	↓ 0.0043	↓ 0.0129	↓ 0.0108
U5	0.047	↓ 0.0081	↓ 0.0041	↓ 0.0124	↓ 0.0104
H1	0.044	↓ 0.0086	↓ 0.0044	↓ 0.0135	↓ 0.011
RRMSE	/	11.78	13.02	10.4	11.06
Models with placed riprap					
P1	0.025	↓ 0.0089	↓ 0.0046	↓ 0.0146	↓ 0.0122
P2	0.022	↓ 0.0085	↓ 0.0044	↓ 0.0135	↓ 0.0113
P3	0.014	↓ 0.0085	↓ 0.0043	↓ 0.0133	↓ 0.0111
P4	0.025	↓ 0.0071	↓ 0.0035	↓ 0.0097	↓ 0.0081
RRMSE	/	16.36	20.82	11.84	13.91
Models with dumped riprap					
D1	0.019	↓ 0.0082	↓ 0.0042	↓ 0.0126	↓ 0.0105
D3	0.022	↓ 0.0068	↓ 0.0034	↓ 0.009	↓ 0.0075
D4	0.042	↓ 0.0089	↓ 0.0046	↓ 0.0146	↓ 0.0121
RRMSE	/	26.43	30.83	21.56	23.86

Table 18 (continued). Breach formation time, t_f (hrs), computed from equations displayed in Table 2 for all three models. The values in light grey and dark grey are respectively the ones contained in a ±30% and ±10% interval centered on the measured value (Table 16). ↓ and ↑ respectively stand for an underestimation and overestimation of the measured value.

Model number	Measured breach formation time	Froehlich (1995b) Eq. 10	Froehlich (2008) Eq. 11	Xu & Zhang (2009) Eq. 12	Froehlich (2016a) Eq. 13
Unprotected models					
CT2	0.05	↓ 0.0137	↓ 0.029	↓ 0.049	↓ 0.028
U1	0.05	↓ 0.0134	↓ 0.0286	↑ 0.0518	↓ 0.027
U2	0.05	↓ 0.0136	↓ 0.029	↑ 0.0517	↓ 0.0275
U3	0.044	↓ 0.0136	↓ 0.029	↑ 0.0506	↓ 0.0276
U4	0.042	↓ 0.0136	↓ 0.029	↑ 0.0503	↓ 0.0276
U5	0.047	↓ 0.0139	↓ 0.0299	↑ 0.0514	↓ 0.028
H1	0.044	↓ 0.014	↓ 0.029	↑ 0.0557	↓ 0.028
RRMSE	/	10.15	5.48	1.92	5.91
Models with placed riprap					
P1	0.025	↓ 0.0143	↑ 0.0305	↑ 0.0513	↑ 0.029
P2	0.022	↓ 0.0144	↑ 0.0307	↑ 0.054	↑ 0.029
P3	0.014	↑ 0.0155	↑ 0.0337	↑ 0.0546	↑ 0.032
P4	0.025	↓ 0.0149	↑ 0.033	↑ 0.0714	↑ 0.031
RRMSE	/	9.67	13.73	43.18	11.99
Models with dumped riprap					
D1	0.019	↓ 0.0146	↑ 0.0316	↑ 0.0578	↑ 0.03
D3	0.022	↓ 0.0161	↑ 0.0363	↑ 0.0757	↑ 0.0344
D4	0.042	↓ 0.014	↓ 0.0296	↑ 0.0506	↓ 0.028
RRMSE	/	20.14	15.82	46.47	15.1

Table 19. Peak outflow, Q_p (m^3/s), computed from equations displayed in Table 3 for all three models. The values in light grey and in dark grey are respectively the ones contained in a ±30% and ±10% interval centered on the measured value (Table 16). ↓ and ↑ respectively stand for an underestimation and overestimation of the measured value.

Model Number	Measured peak outflow	Soil Conservation Service (1981) Eq. 14	Singh & Snorrason (1982) Eq. 15	Singh & Snorrason (1984) Eq. 16	MacDonald & Langridge-Monopolis (1984) Eq. 17	U.S. Bureau of Reclamation (1982) Eq. 18	Costa (1985) Eq. 19	Costa (1985) Eq. 20	Evans (1986) Eq. 21	Froehlich (1995b) Eq. 22
Unprotected models										
CT2	0.141	↑ 7.48	↑ 13.4	↑ 7.2	↑ 2.73	↑ 8.61	↑ 4.72	↑ 2.83	↑ 2.74	↑ 0.75
U1	0.112	↑ 6.63	↑ 13.4	↑ 7.18	↑ 2.59	↑ 7.64	↑ 4.55	↑ 2.75	↑ 2.65	↑ 0.68
U2	0.122	↑ 6.65	↑ 13.4	↑ 7.2	↑ 2.59	↑ 7.65	↑ 4.55	↑ 2.75	↑ 2.65	↑ 0.68
U3	0.112	↑ 7	↑ 13.4	↑ 7.18	↑ 2.66	↑ 8.05	↑ 4.64	↑ 2.79	↑ 2.69	↑ 0.71
U4	0.122	↑ 7.06	↑ 13.4	↑ 7.18	↑ 2.66	↑ 8.12	↑ 4.64	↑ 2.79	↑ 2.69	↑ 0.71
U5	0.148	↑ 6.57	↑ 13.4	↑ 7.18	↑ 2.55	↑ 7.56	↑ 4.46	↑ 2.71	↑ 2.6	↑ 0.67
H1	0.161	↑ 7.7	↑ 13.4	↑ 7.2	↑ 2.77	↑ 8.86	↑ 4.77	↑ 2.85	↑ 2.76	↑ 0.77
RRMSE	/	750.9	1 445.41	768.78	274.48	866.25	488.94	288.74	278.01	63.14
Models with placed riprap										
P1	0.389	↑ 8.86	↑ 18.91	↑ 7.76	↑ 2.91	↑ 10.19	↑ 4.9	↑ 3.14	↑ 2.84	↑ 0.85
P2	0.387	↑ 7.7	↑ 18.03	↑ 7.66	↑ 2.74	↑ 8.86	↑ 4.7	↑ 3	↑ 2.73	↑ 0.76
P3	0.459	↑ 7.48	↑ 18.32	↑ 7.66	↑ 2.7	↑ 8.61	↑ 4.65	↑ 3	↑ 2.7	↑ 0.74
P4	0.241	↑ 4.16	↑ 18.91	↑ 7.76	↑ 2.07	↑ 4.78	↑ 3.86	↑ 2.63	↑ 2.27	↑ 0.45
RRMSE	/	466.81	1 231.61	497.42	152.47	540.83	282.64	174.58	153.89	23.33
Models with dumped riprap										
D1	0.277	↑ 6.75	↑ 18.91	↑ 7.76	↑ 2.58	↑ 7.77	↑ 4.5	↑ 2.95	↑ 2.62	↑ 0.68
D3	0.238	↑ 3.63	↑ 18.91	↑ 7.76	↑ 1.95	↑ 4.18	↑ 3.7	↑ 2.55	↑ 2.18	↑ 0.41
D4	0.202	↑ 8.81	↑ 18.03	↑ 7.7	↑ 2.91	↑ 10.14	↑ 4.9	↑ 3.11	↑ 2.84	↑ 0.85
RRMSE	/	909.24	2 563.71	1 046.17	317.71	1 051.28	580.05	368.54	324.3	62.99

Table 19 (continued). Peak outflow, Q_p (m^3/s), computed from equations displayed in Table 3 for all three models. The values in light grey and dark grey are respectively the ones contained in a ±30% and ±10% interval centered on the measured value (Table 16). ↓ and ↑ respectively stand for an underestimation and overestimation of the measured value.

Model Number	Measured peak outflow	Walder & O'Connor (1997) Eq. 23	Walder & O'Connor (1997) Eq. 24	Walder & O'Connor (1997) Eq. 25	Pierce (2008) Eq. 26	Pierce (2008) Eq. 27	Pierce (2008) Eq. 28	Pierce (2008) Eq. 29	Xu & Zhang (2009) Eq. 30	Froehlich (2016b) Eq. 31
Unprotected models										
CT2	0.141	↑ 3.7	↑ 0.91	↑ 1.5	↓ 0.06	↓ 0.08	↑ 0.25	↓ 0.06	↓ 0.11	↓ 0.12
U1	0.112	↑ 3.59	↑ 0.78	↑ 1.42	↓ 0.06	↓ 0.07	↑ 0.21	↓ 0.06	↓ 0.1	↓ 0.11
U2	0.122	↑ 3.59	↑ 0.79	↑ 1.42	↓ 0.06	↓ 0.07	↑ 0.21	↓ 0.06	↓ 0.1	↓ 0.11
U3	0.112	↑ 3.65	↑ 0.84	↑ 1.46	↓ 0.06	↓ 0.07	↑ 0.23	↓ 0.06	↓ 0.1	↑ 0.12
U4	0.122	↑ 3.65	↑ 0.85	↑ 1.46	↓ 0.06	↓ 0.07	↑ 0.23	↓ 0.06	↓ 0.1	↓ 0.12
U5	0.148	↑ 3.54	↑ 0.77	↑ 1.39	↓ 0.06	↓ 0.07	↑ 0.21	↓ 0.06	↓ 0.09	↓ 0.11
H1	0.161	↑ 3.73	↑ 0.95	↑ 1.52	↓ 0.06	↓ 0.08	↑ 0.26	↓ 0.06	↓ 0.09	↓ 0.12
RRMSE	/	381.81	77.61	144.04	7.98	6.55	10.77	7.98	4.24	2.53
Models with placed riprap										
P1	0.389	↑ 3.81	↑ 1.13	↑ 1.6	↓ 0.07	↓ 0.09	↓ 0.32	↓ 0.06	↓ 0.13	↓ 0.15
P2	0.387	↑ 3.68	↑ 0.95	↑ 1.5	↓ 0.06	↓ 0.08	↓ 0.26	↓ 0.06	↓ 0.11	↓ 0.13
P3	0.459	↑ 3.66	↑ 0.91	↑ 1.48	↓ 0.06	↓ 0.08	↓ 0.25	↓ 0.06	↓ 0.11	↓ 0.12
P4	0.241	↑ 3.14	↑ 0.43	↑ 1.12	↓ 0.04	↓ 0.05	↓ 0.11	↓ 0.05	↓ 0.06	↓ 0.08
RRMSE	/	217.43	35.61	72.02	21.65	20.43	9.68	21.71	18.5	17.41
Models with dumped riprap										
D1	0.277	↑ 3.56	↑ 0.8	↑ 1.41	↓ 0.06	↓ 0.07	↓ 0.21	↓ 0.06	↓ 0.1	↓ 0.12
D3	0.238	↑ 3.04	↑ 0.37	↑ 1.05	↓ 0.04	↓ 0.04	↓ 0.09	↓ 0.04	↓ 0.06	↓ 0.07
D4	0.202	↑ 3.81	↑ 1.12	↑ 1.6	↓ 0.07	↓ 0.09	↑ 0.31	↓ 0.06	↓ 0.13	↓ 0.15
RRMSE	/	452.99	85.74	158.97	25.93	24.77	15.71	26.27	21.03	18.98

4.5 Discussion of the results

4.5.1 Suitability of breach width equations

The protected models' breach width could not be determined since the entire width of the materials was carried away downstream during the breaching, indicating that the breach width exceeds the flume width. Unfortunately, for model CT2, the breach width could not be estimated either. This is to be imputed to one camera on the downstream face being slightly displaced and allowing only two ground control points to be visible, providing a less accurate georeferencing.

For the other unprotected models, the breach widths could be obtained (Table 17). The estimations provided by Eq. (1) (U.S. Bureau of Reclamation, 1988) overestimate quite significantly the measured values. Indeed, this equation was developed for earthfill dams, the obtained results are then following what could be expected from the large breaching of an earthen hydraulic work. In comparison, Eq. (2) (U.S. Bureau of Reclamation, 1988) was developed for rockfill dams and provide better results, even though the estimations are still greater than what is observed from the breached models. The best estimations are made for models that underwent high overtopping discharge values (U3, U5, and H1, with respectively 10, 15, and 15 $l.s^{-1}$, see Table 14). Eq. (2) may better fit an overtopping with a sudden and high level of discharge, similar to a disastrous flood. The objective of the U.S. Bureau of Reclamation (1988) is to determine the hazard classification of dams, and this equation is consistent with it, providing conservative results.

When the critical discharge level is less important, the breach width tends to be smaller (models U1, U2, and U4 with an overtopping discharge of 5 $l.s^{-1}$) and Eq. (5) (Xu & Zhang, 2009) appears to propose a reasonable estimation, even though it still underestimates the values slightly. However, the equation does not provide a good estimation of the breach width for the only homogeneous model without a core that we have (H1) despite that the equation considers design specificity. Froehlich equations (1995a, 2008, and 2016a) also tend to underestimate the breach values, but even more than Eq. (5) (Xu & Zhang, 2009). However, the most recent equation (Eq. 6) provides greater values than the former ones (Eqs. 3 and 4) and tends to get closer to the measured width.

4.5.2 Suitability of failure time equations

Contrary to the breach width, the failure times could be estimated for all 14 models (Table 18). From these estimations, it appears that Eqs. 7, 8 (MacDonald & Langridge-Monopolis, 1984), and 9 (U.S. Bureau of Reclamation, 1988) are underestimating the failure times. The only exception is for model P3 where Eq. 9 provides a quite good estimation of the failure time. As for the breach width estimations, the conservative results obtained from the U.S. Bureau of Reclamation (1988) are consistent with the objective of such a report. It is of interest to highlight the good repeatability of the results obtained for unprotected models. Indeed, for all of them, only Eq. 12 (Xu & Zhang, 2009) provides very good failure time estimations. Whether the unprotected models are with core walls (rubber core or XPS foam rectangles) or without core (model H1). The equations 10, 11, and 13 from Froehlich (1995b, 2008 and 2016a) underestimate the failure time for unprotected models, even though Eq. 11 and 13 tend to display values closer to the measured failure times than Eq. 10.

For protected models, it seems that no equation provides a good estimation of the time failure for all of them. It can be noticed that Eq. 10 (Froehlich, 1995b) is the only equation able to correctly estimate the failure times for dumped riprap model with a thick layer of riprap (models D1 and D3). However, the characterization is quite bad for a thinner layer of riprap (model D4). Froehlich (2016a) may be the one providing the closest results for placed riprap, but it remains difficult to clearly state which equation is the best. These results highlight the fact that a difference in design (placed or dumped riprap, size of the pilot channel) can have an impact on the failure time and the validity of the parametric breaching equations. Also, we can notice that contrary to unprotected models, Eqs. 11-13 (Froehlich, 2008; Xu & Zhang, 2009; Froehlich, 2016a) tend to overestimate the failure times for both placed and dumped riprap models. Particularly Eq. 12 (Xu & Zhang, 2009) which can correctly estimate the unprotected model's failure time but is overestimating by far the ones for protected models.

4.5.3 Suitability of peak outflow equations

As for the failure times, the peak outflows could be estimated for all 14 models (Table 19). From these results, it can be observed that the oldest references with Eqs. 14 -21, 23, 25 (Soil Conservation Service, 1981; Singh & Snorrason, 1982 and 1984; MacDonald & Langridge-Monopolis, 1984; U.S. Bureau of Reclamation, 1982; Costa, 1985; Evans, 1986; Walder &

O'Connor, 1997) greatly overestimates the peak outflows. On the other hand, Pierce's (2008) equations (Eqs. 26, 27, and 29) underestimate the peak outflow values. However, as for the estimation of failure times, the results highlight the suitability of one specific reference, Eq. 31 (Froehlich, 2016b) for all unprotected models. Eq. 30 (Xu & Zhang, 2009) also displays good results for the characterization of peak outflow for unprotected models, except for models U5 and H1. These two models are the ones that were exposed to a higher level of inflow (Table 14), suggesting that Eq. 30 is less able to characterize peak outflow values for greater discharges than the ones that could be observed during disastrous floods.

For protected models, no parametric equation appears to suit the estimation of peak outflow. The peak outflows for such models are much more important than for the unprotected ones. Thus, Eqs. 30 and 31 (Xu & Zhang, 2009; Froehlich, 2016b) underestimate the peak outflow, except Eq. 31 for model D4 which has a thinner layer of dumped riprap. Eq. 28 (Pierce, 2008), using h_w as an input parameter, appears to be the best equation for estimating peak outflow values for protected models even though its ability to characterize peak outflow is more or less pertinent according to the dam design (width or absence of pilot channel and thickness of riprap layer). The peak outflows from models P4 and D3 could not be estimated correctly because of low h_b, h_w, $W_{avg,}$ and V_w values for these two models (Table 15). They are imputed to i) the lack of fiber cloth for model P4, inducing an early rupture in comparison to the other placed riprap models; and to ii) a breaching in two sequences for model D3, with a first small slide of the riprap early on, reducing the dam elevation before the real failure occurs (Figure 25).

4.5.4 Limitations

After going through the analysis of the results provided by the parametric equations for the estimation of B_{avg}, $t_{f,}$ and Q_p, some limitations need to be pointed out. First, from all the references considered in this research work, it is rarely mentioned if the dam failure cases used to establish the relations are protected by riprap or not. The impact of the type of riprap structure (placed or dumped) has never been investigated. This lack of consideration for protective layers is striking from the results displayed in Tables 17, 18, and 19. Indeed, no equation can characterize the failure times and peak outflows for all protected models, or even for one specific type of riprap. The characterization of breaching parameters for placed riprap dams is particularly difficult since they undergo a different failure mechanism (sudden

sliding) than the other dam designs. Likewise, apart from the U.S. Bureau of Reclamation (1988), no parametric equation is dedicated to the estimation of breaching parameters for rockfill dams exclusively. Furthermore, when the equations should be representative of embankment dams, the historical failure cases considered are mostly earthfill dams instead of rockfill ones.

Also, this work highlights that the parametric equations providing the best suitability to the values measured on the experimental models are the ones that considered a large number of failure cases to be established. Thus, the works considering the greatest number of failure cases are Froehlich (2016a) and Xu & Zhang (2009) with respectively 111 and 182 dam cases used and they appear to display better suitability. However, references with fewer failure cases such as Soil Conservation Service (1981), Singh & Snorrason (1982) and (1984), MacDonald & Langridge-Monopolis (1984), U.S. Bureau of Reclamation (1982), Costa (1985), Evans (1986) and Walder & O'Connor (1997) were unable to correctly characterize none of the breaching parameters obtained from our experimental tests.

Limitations from the experimentations should as well be mentioned here. As a matter of fact, a limiting aspect of this research is the number of tests that were carried out. Fourteen tests cannot pretend to be representative enough to do a proper statistical analysis. Also, the results obtained limit themselves to the very specific properties of the models: steep upstream and downstream slopes, specific material properties (size and density), and riprap stone positioning. The representativity of the rubber core and XPS foam rectangles to stand as core walls could also be discussed and criticized.

The dimension of the facility available in the hydraulic laboratory is also a point of discussion. First, the reservoir size is quite small in comparison to what can be observed at the prototype scale. Consequently, the breach development will stabilize before reaching the bottom of the model. Another limit that can be pointed out is the limited width of the flume (1 m) which does not allow to study the breach width development for protected models. A larger flume could have enabled a deeper study on that specific point.

5 Concluding summary

This research report aimed at achieving a better understanding of breach development of embankment dams exposed to overtopping from laboratory experiments, prototype dams, and historical failure cases. The parametric breach models were detailed for three breaching parameters: breach width, breach formation time, and peak outflow.

This research report aimed to compare the ability of the parametric breach models to estimate the measured breaching parameters from all dam cases, according to the input parameters and the type of design. Two different studies were carried out successively at two different scales. Firstly, three prototype embankment dams, taken from the IMPACT project, and five historical failure cases of embankment dams were considered. Then, fourteen laboratory experimental models, unprotected or with placed or dumped riprap were studied. All these cases underwent a failure process due to overtopping.

The properties of all experimental and prototype dams' constitutive materials, as well as the input parameters required for the use of parametric breach models, were introduced. Furthermore, parametric breaching equations were displayed for the estimation of breach width, breach formation time, and peak outflow, with the associated types of dams they correspond to. The measured and estimated breaching parameter values were then displayed and discussed.

The results suggest that the ability of the different parametric models to estimate a breaching parameter depends a lot on the dam and reservoir characteristics. Also, the results obtained at the experimental scale do not necessarily coincide with the ones obtained at the prototype scale. It is important to highlight that parametric breach models developed from embankment dam data were mainly considering earthfill dam cases but very few rockfill dams. However, we were able to point out the most suitable equations from the different ones available in the literature. We must highlight that the validity of our results is limited to the tests and cases displayed in this research work.

For the estimation of the breach width (B_{avg}), Xu & Zhang (2009) and Froehlich (2016a) appear to provide the best estimations from the prototype dams and historical failure cases, taking into consideration all types of embankment structures. However, for the laboratory dams without protection, the U.S Bureau of Reclamation (1988) model made up for rockfill

dams provides the best characterization, and a reasonable estimation of the breach width for rockfill prototype dams as well.

For estimating the breach formation time (t_f), it is quite striking that Xu & Zhang (2009) provide the best results for unprotected rockfill dams built in the laboratory. Nevertheless, models proposed by Froehlich (1995, 2008, and 2016a) give the best estimations for protected laboratory models and all types of embankment dams at the prototype scale.

Froehlich (2016b) proposes the best estimation of peak outflow (Q_p) but mostly for bigger reservoirs looking at prototype dams and historical failure cases. From the experimental rockfill models, Froehlich's (2016b) model also provides very good estimations, along with Xu & Zhang (2009). However, the quality of these estimations only stands for unprotected dams. Indeed, protected models (dumped or placed riprap) were poorly characterized.

Finally, for the prototype models, the results obtained with the use of a simplified physical model (DLBreach) enhance its ability to take into consideration much more information on the material properties and inflow variations, enabling a much better estimation of the breaching parameters for all prototype dams (both earthfill and rockfill). The big variations of results obtained from parametric breach models according to the type of dam, design, and reservoir dimensions finally suggest the use of a simplified physical model instead, when enough data is available.

Acknowledgment

Chapter 4 bases on a publication co-authored by Geir Helge Kiplesund. The important contribution from Geir Helge Kiplesund is gratefully acknowledge, but the laboratory tests described in Chapter 4 were carried out as a part of his PhD study. We also thank the authors of the MSc thesis at NTNU on breaching of rockfill dam, these are: Styrmir Sigurjónsson, Ghaith Alkholossi, Nisal D. H. A. Senarathna, Raj Kumar Kc and Saroj Sapkota.

The experimental work presented was carried out as a part of Work Package 1, Project 1.2 Dam Construction and Dam Safety within HydroCen, Norway.

The writing of this report is made possible with the financial support offered by the Norwegian Water Resources and Energy Directorate (NVE), Hafslund E-CO Vannkraft, Hydro Energi, NEAS, SFE Produksjon, Sira-Kvina, Skagerak Kraft AS, Statkraft, Tafjord Kraftproduksjon, and Trønder Energi, all in Norway.

References

Abt, S. R., & Johnson, T. L. (1991). Riprap design for overtopping flow. *Journal of hydraulic engineering*, *117*(8), 959-972.

Abt, S. R., Thornton, C. I., Scholl, B. A., & Bender, T. R. (2013). Evaluation of overtopping riprap design relationships. *JAWRA Journal of the American Water Resources Association*, *49*(4), 923-937.

Abt, S.R.; Thornton, C.I. Riprap Design for Overtopping—Man Do I Need a Martini! (2014). *World Environ. Water Resour. Congr.* 191–1198.

Aldridge, B. N. (1987). U.S. Geological Survey, written communication.

Costa, J. E. 1985. Floods from dam failures. *U.S. Geological Survey Open-File Report.* Denver. 54.

Courivaud, J. R. (2007). Analysis of the dam breaching database. CEATI Rep. No. T032700-0207B, CEATI International, Dam Safety Interest Group, Montréal.

Dezert, T., Kiplesund, G. H., & Sigtryggsdóttir, F. G. (2022). Riprap Protection Exposed to Overtopping Phenomena: A Review of Laboratory Experimental Models. *Water*, *14*(17), 2722.

Dezert, T., & Sigtryggsdóttir, F. G. (2024a). Evaluation of Parametric Breach Models from Prototype and Historical Embankment Dams under Overtopping Conditions. *Journal of Geotechnical and Geoenvironmental Engineering*, *150*(4), 04024015.

Dezert, T., & Sigtryggsdóttir, F. G. (2024b). Stability evaluation of toe supported ripraps exposed to overtopping: report R&D-project 80418, part 1. NVE Ekstern rapport nr. 12/2024.

Dezert, T., Kiplesund, G. H., & Sigtryggsdóttir, F. G. (2024). Parametric breach model evaluation from laboratory rockfill dam models under overtopping conditions. *Journal of Hydraulic Engineering, 150(6)*, https://doi.org/10.1061/JHEND8.HYENG-1401.

EBL Kompetanse. (2006). Stability and breaching of embankment dams. Rep. Sub-project 3 (SP3): Breaching of embankment dams, Norway.

Evans, S. G. 1986. The maximum discharge of outburst floods caused by the breaching of man-made and natural dams. *Can. Geotech. J.* 23(3). 385–387.

Froehlich, D. C. 1995a. Embankment dam breach parameters revisited. *International Water Resources Engineering Conference - Proceedings* 1. 887–891.

Froehlich, D. C. 1995b. Peak outflow from breached embankment dam. *Journal of Water Resources Planning and Management* 121(1). 90–97.

Froehlich, D. C. 2008. Embankment dam breach parameters and their uncertainties. *Journal of Hydraulic Engineering* 134(12). 1708–1721.

Froehlich, D. C. 2016a. Empirical model of embankment dam breaching. *River Flow 2016*. CRC Press.

Froehlich, D. C. 2016b. Predicting peak discharge from gradually breached embankment dam. *Journal of Hydrologic Engineering* 21(11). 04016041.

Fujia, T., and Yumei, L. (1994). Reconstruction of Banqiao and Shimantan dams. *Int. J. Hydropower Dams,* 1(4), 49–53.

Henan Water Resources Authority. (2005). The August 1975 catastrophic flood disaster in Henan, *Yellow River Water Conservancy Press*, Zhenzhou, China.

Hiller, Priska H, Aberle, J., & Lia, L. (2018). Displacements as failure origin of placed riprap on steep slopes. *Journal of Hydraulic Research*, *56*(2), 141–155.

Hiller, P. H., Lia, L., & Aberle, J. (2019). Field and model tests of riprap on steep slopes exposed to overtopping. *Journal of Applied Water Engineering and Research*, 7(2), 103-117.

International Commission on Large Dams. (1974). Lessons from dam incidents, complete Ed., Paris.

International Commission on Large Dams (ICOLD). Dam Failures Statistical Analysis. Bulletin 99. 1995. Available online: https://www.icold-cigb.org/GB/publications/bulletins.asp (accessed on 31 August 2022).

ICOLD. 2020. ICOLD World Register of Dams - General Synthesis Available online: https://www.icold-cigb.org/GB/world_register/general_synthesis.asp (accessed on Sep 26, 2022).

ICOLD. Dam Failures—Statistical Analysis; Bulletin 188; ICOLD: Paris, France, (2021).

Jansen, R. B. (1983). Dams and public safety, U.S. Department of the Interior, Bureau of Reclamation, Denver.

Khan, D., & Ahmad, Z. (2011). Stabilization of angular-shaped riprap under overtopping flows. *World Academy of Science, Engineering and Technology*, *59*, 1153-1157.

Kiplesund, G. H., Ravindra, G. H., Rokstad, M. M., & Sigtryggsdóttir, F. G. (2021). Effects of toe configuration on throughflow 572 properties of rockfill dams. *Journal of Applied Water Engineering and Research*, *9*(4), 277-292.

Kiplesund, G. H., Sigtryggsdottir, F. G., & Lia, L. (2023). Breach Progression Observation in Rockfill Dam Models Using Photogrammetry. *Remote Sensing*, *15*(6). 1715.

MacDonald, T. C., & Langridge-Monopolis, J. 1984. Breaching characteristics of dam failures. *Journal of Hydraulic Engineering*, *110*(5), 567-586.

McEwen, K. (1991). Report on Cougar Creek dam failure. *Engineering Rep.*, Alberta Environment, Water Resources Management Services, Dam Safety Branch, Ala., Canada.

Morris, M., Hassan, M., Kortenhaus, A. & Visser, P. 2009. Breaching processes: A state of the art review. Technical report. *FLOODsite.*

Morris, M. (2009). Breach initiation and growth: Physical processes. Project Floodsite. Report T06-08-11. *HR Wallingford.*

Najafzadeh, M.; Oliveto, G. (2020). Riprap incipient motion for overtopping flows with machine learning models. *J. Hydroinformatics*, *22*, 749–767.

NVE. 2012. Veileder for fyllingsdammer. Report n. 4/2012. Nor. Water Resour. Energy Dir. (2012), 21–25. Available online: https://publikasjoner.nve.no/veileder/2012/veileder2012_04.pdf

Olivier, H. (1967) Through and Overflow Rockfill Dams-New Design Techniques. *Proc. Inst. Civ. Eng. 36*, 433–471.

Pierce, M. W. 2008. Predicting peak outflow from breached embankment dams. MS thesis. *Colorado State Univ. Fort Collins, Colo*

Qing, D. (1998). The river dragon has come!: The Three Gorges Dam and the fate of China's Yangtze River and its people, M. E. Sharpe, Armonk, NY.

Ravindra, G.H.R. Hydraulic and Structural Evaluation of Rockfill Dam Behavior When Exposed to Throughflow and Overtopping Scenarios. (2020). Ph.D. Thesis, Norwegian University of Science and Technology, Trondheim.

Ravindra, G.H.R.; Gronz, O.; Dost, B.; Sigtryggsdóttir, F.G. Description of failure mechanism in placed riprap on steep slope with unsupported toe using smartstone probes. Eng. Struct. (2020), 221, 111038, doi:10.1016/j.engstruct.2020.111038.

Ravindra, G. H. R., & Sigtryggsdottir, F.G. (2021). Rockfill dams – downstream riprap and dam toe: FoU-project 80409. NVE Ekstern rapport nr. 17/2021.

Siebel, R. (2007). Experimental investigations on the stability of riprap layers on overtoppable earthdams. *Environmental fluid mechanics*, *7*(6), 455-467.

Singh, K. P. & Snorrason, A. 1982. 'Sensitivity of outflow peaks and flood stages to the selection of dam breach parameters and simulation models', State Water Survey (SWS) Contract Rep. No. 288. Illinois Dept. of Energy and Natural Resources, SWS Div., Surface Water at the University of Illinois.

Singh, K. P., & Snorrason, A. 1984. Sensitivity of outflow peaks and flood stages to the selection of dam breach parameters and simulation models. *Journal of hydrology*, *68*(1-4), 295-310.

Soil Conservation Service (SCS). 1981. "Simplified dam-breach routing procedure. Technical Release Rep. No. 66 (Rev. 1).

Stephenson, D.J. (1979). *Rockfill in Hydraulic Engineering*; Elsevier: Amsterdam, The Netherlands.

Thornton, C. I., Abt, S. R., Scholl, B. N., & Bender, T. R. (2014). Enhanced stone sizing for overtopping flow. *Journal of hydraulic engineering*, *140*(4), 06014005.

U.S. Bureau of Reclamation. 1982. Guidelines for defining inundated areas downstream from Bureau of Reclamation dams. Reclamation Planning Instruction Rep. No. 82-11.

U.S. Bureau of Reclamation. 1988. Downstream hazards classification guidelines. Technical Report 11. Department of the Interior. Denver, CO.

Vaskinn, K. A., Lovoll, A. & Höeg, K. (2004), Wp2.1 breach formation - large scale embankment failure, Technical Report 1, IMPACT.

Walder, J. S. & O'Connor, J. E. 1997. Methods for predicting peak discharge of floods caused by failure of natural and constructed earthen dams. *Water Resources Research* 33(10). 2337–2348.

Wu, W. (2016), Introduction to dlbreach - a simplified physically-based dam/levee breach model, Technical report, Clarkson University, Box 5710, 8 Clarkson Avenue Potsdam, NY 13699, USA. (Version 2016.4).

Xu, Y., Zhang, L., and Jia, J. (2008). Lessons from Catastrophic Dam Failures in August 1975 in Zhumadian, China. *Geocongress 2008: Geosustainability and geohazard mitigation*, K. R. Reddy, M. V. Khire, and A. N. Alshawabkeh, eds., ASCE, Reston, VA, 162–169.

Xu, Y. & Zhang, L. M. (2009). Breaching parameters for earth and rockfill dams. *Journal of Geotechnical and Geoenvironmental Engineering* 135(12). 1957–1970.

Xu, Y., Zhang, L., and Jia, J. (2009). Catastrophic failure of Banqiao Dam. Proc., Case Studies: Learning from Dam Incidents and Failures, Centre for Energy Advancement through Technological Innovation (CEATI) International, Montreal, 24–25.

Zhong, Q., Wu, W., Chen, S., & Wang, M. (2016). Comparison of simplified physically based dam breach models. *Natural Hazards*, *84*, 1385-1418.

Appendix A

Generally accepted principles to evaluate and model the flow through and over a riprap on steep slopes are not yet formulated. Due to high turbulence and a free water surface, Froude's model law can be used to scale the critical discharge values measured for each overtopping test. For all rockfill dam models, a 1:10 scale is considered. The scaled dischare values are displayed in Table A.1, for a 1 m width section of a 10 meters width dam, with corresponding references and number of tests carried out.

Table A.1. Scaled discharge values for all rockfill dam models overtopped in NTNU hydraulic laboratory, for a 1 m width section of a 10 meters width dam.

Model description	q_c ($m^2.s^{-1}$)	Δq ($m^2.s^{-1}$)	Quantity of tests	References
Half dam – No toe support				
Unprotected – No toe	1.21	0.27	3	Kiplesund et al. (2021)
Unprotected – External toe	1.48	0.27	3	Kiplesund et al. (2021)
Unprotected – Internal toe	1.42	0.07	3	Kiplesund et al. (2021)
Unprotected – Combined toe	1.05	0.15	3	Kiplesund et al. (2021)
Dumped riprap – No toe	5.53	0.79	2	Ravindra and Sigtryggsdóttir (2021)
Dumped riprap – Internal toe	8.7	0.79	2	Ravindra and Sigtryggsdóttir (2021)
Placed riprap – No toe	9.49	0	2	Ravindra and Sigtryggsdóttir (2021)
Placed riprap – Internal toe	14.23	0	2	Ravindra and Sigtryggsdóttir (2021)
Half dam – Toe support				
Placed riprap – No toe	31.62	7.91	2	Dezert et al. (2023)
Full dam – No toe support				
Unprotected – No core	5.14	0.68	4	Dezert et al. (2024)
Unprotected – Rubber core	2.56	1.24	5	Dezert et al. (2024)
Dumped riprap – Rubber core	7.91	1.58	2	Dezert et al. (2024)
Placed riprap – Rubber core	15.28	1.97	3	Dezert et al. (2024)

NVE

Norges vassdrags- og energidirektorat

Middelthuns gate 29
Postboks 5091 Majorstuen
0301 Oslo
Telefon: (+47) 22 95 95 95